Icy satellites: Interior structure, dynamics and evolution

Francis Nimmo, University of California Santa Cruz

Summary

This article consists of three sections. The first discusses how we determine satellite internal structures, and what we know. The primary probes of internal structure are measurements of magnetic induction, gravity and topography, and rotation state and orientation. Enceladus, Europa, Ganymede, Callisto, Titan and (perhaps) Pluto all have subsurface oceans; Callisto and Titan may be only incompletely differentiated. The second section describes dynamical processes that affect satellite interiors and surfaces: tidal and radioactive heating, flexure and relaxation, convection, cryovolcanism, true polar wander, non-synchronous rotation, orbital evolution and impacts. The final section discusses how the satellites formed and evolved. Ancient tidal heating episodes and subsequent refreezing of a subsurface ocean are the likeliest explanation for the deformation observed at Ganymede, Tethys, Dione, Rhea, Miranda, Ariel and Titania.The high heat output of Enceladus is a consequence of Saturn's highly dissipative interior, but the dissipation rate is strongly frequency-dependent and does not necessarily imply that Saturn's moons are young. Major remaining questions include the origins of Titan's atmosphere and high eccentricity, the regular density progression in the Galilean satellites, and the orbital evolution of the Saturnian and Uranian moons.

Keywords: Tides, satellites, orbits, tectonics, dissipation, convection, gravity, topography, flexure

**Main text**

The icy bodies of the outer solar system present a fascinating and diverse picture (Figure 1). From tiny, active Enceladus, to Titan with its unique atmosphere, to Pluto's nitrogen glaciers, there is an astonishing variety on display. The aim of this article is to describe some of that variety, and to attempt to explain how it came about.

This article will focus in particular on the interiors of these bodies: what their internal structures are (Section 1), what processes are operating (Section 2), and how they have evolved over time (Section 3). Particular attention is paid to bodies which are thought to have subsurface oceans, because these potentially-habitable environments are high-priority targets for future spacecraft missions. Although Pluto is not a satellite, it is an icy world and as such it is included; but Ceres, a volatile-rich asteroid, is not.

At the start of each section some review articles which go into greater depth than this article are noted. There are also entire books devoted to particular icy satellites, notably Europa (Pappalardo et al. 2009), Titan (Muller-Wodarg et al. 2014) and Enceladus (Schenk et al. 2018).

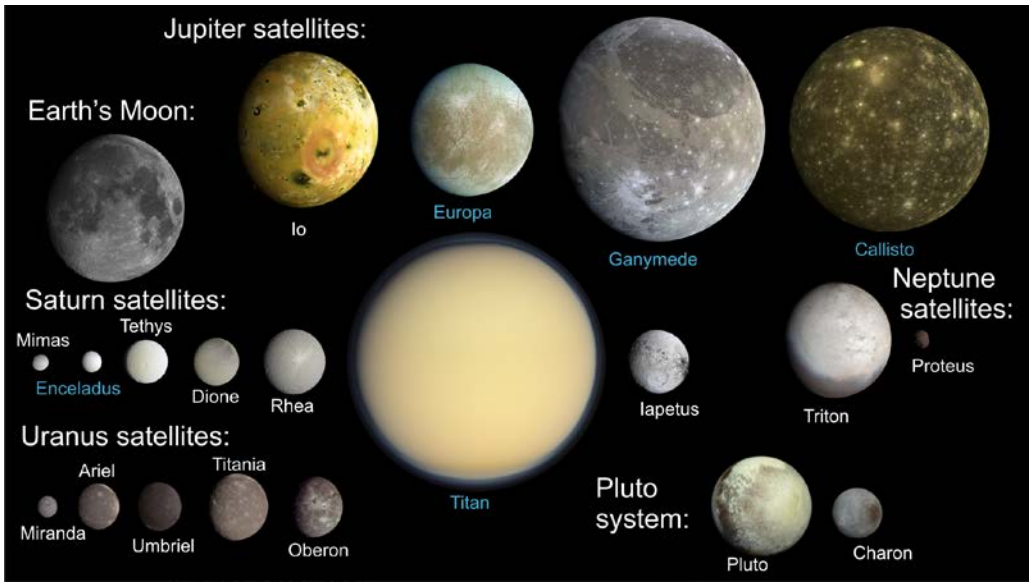


**Figure 1**. (Mostly) icy worlds of the outer solar system, with the Earth's moon to scale. Names in blue are bodies likely to possess subsurface oceans. From Nimmo & Pappalardo (2016).

## 1. Interior Structure

Deducing the internal structure of a body from remote observations is a challenging task. This section will first discuss how it is done (Section 1.1), and then describe what we have learnt (Section 1.2). One key question is whether the icy satellites are differentiated, i.e. separated into silicate-dominated and ice-dominated layers. This is important because it places constraints on how they originally formed (Section 3.2). Another important topic is sub-surface oceans – how they are detected, and how they are maintained. Many review articles cover similar topics, including Hussmann et al. (2006) and Nimmo & Pappalardo (2016) for generic satellites, and chapters by Schubert et al. (2004) for the Galilean satellites, Tobie et al. (2014) for Titan, and Hemingway et al. (2018) for Enceladus.

Before describing how interior structures are deduced, two topics are introduced – the physical properties of ice, and the role of tides - because they are fundamental to everything discussed below.

*Ice properties*. Just like rock, ice at the surface is cold and will respond to stresses in a brittle or elastic fashion (Section 2.1.3). At higher temperatures and depths, it will flow viscously, potentially leading to convection (Section 2.1.4). Unlike rock, the low-pressure phase of water ice (ice I) is *less* dense than its liquid equivalent, while the same is not true of the ice polymorphs that form at higher pressures (Sotin et al. 1998). As a result, a generic large satellite will consist of an "ice sandwich": ice I on top, water in the middle, higher-pressure ice polymorphs beneath. A progressively freezing ocean in this situation will freeze simultaneously from the top and bottom. Smaller satellites will not have high-P ice phases, because these only appear above ~0.2 GPa. In the absence of high-P ices, the volume change of water to ice results in expansion of the surface (potentially causing extensional surface tectonics; Nimmo 2004) and pressurization of the ocean (potentially causing eruptions; Manga & Wang 2007). Although the freezing point of water is not very sensitive to pressure, it is quite sensitive to the concentration of contaminants: salts can lower the freezing point by tens of K, and in the presence of $NH_3$ the freezing point may be as

low as 176 K (Kargel 1998, Leliwa-Kopystynski et al. 2002). Because freezing excludes contaminants, the remaining liquid becomes progressively more contaminated and thus harder to freeze.

*Tides*. Tides dominate much of satellite dynamics; an accessible introduction to them is found in Chapter 4 of Murray and Dermott (1999). Almost all satellites are synchronous, rotating once per orbit. The mean shape of such a satellite is an ellipsoid elongated towards the primary; this shape results from tidal and rotational distortions. If the orbit is non-circular with an eccentricity *e*, from the satellite's point of view the primary executes an ellipse in the sky (Figure 2). The changing distance and direction of the primary exert torques on the satellite. They also cause small periodic changes to the equilibrium ellipsoidal shape, resulting in so-called diurnal tides. This diurnal tidal deformation is much smaller (by a factor of 3*e*) than the equilibrium ellipsoidal shape, but its time-varying nature causes stresses, and for a non-rigid body can also generate heat. A similar process arises if the satellite has a finite obliquity (i.e. its spin pole is at an angle to its orbit pole). This tidal heating is the prime driver of geological activity on the icy satellites (Section 2.1.2). The heating rate is strongly dependent on satellite interior structure, orbital eccentricity and distance to the primary, and varies spatially over the satellite. Eccentricity tidal heating progressively circularizes a satellite's orbit, so that there is an intricate feedback between orbital and thermal evolution (Section 3.1.2).

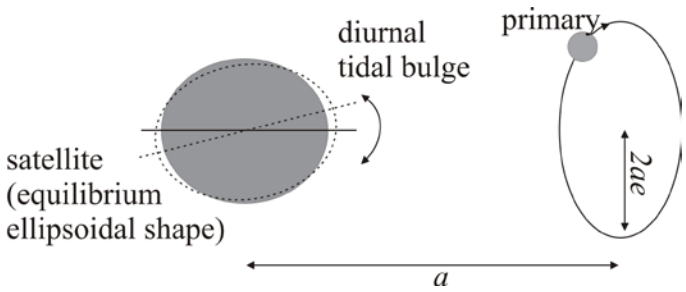


**Figure 2.** Schematic of satellite tides. Viewed in the satellite's reference frame the primary executes an ellipse; the diurnal component of the tidal bulge tracks the position of the primary.

*1.1 How do we know?*

For the icy satellites there are several kinds of observations which can place constraints on their internal structures.

*1.1.1 Bulk density.* Even a single flyby of a moon will usually yield its mass (by measuring perturbations to the spacecraft) and its volume (via images). The resulting bulk density gives no information on how mass is distributed within the satellite. Nonetheless, it can still be useful, because rock/metal mixtures have densities of 3-4 g/cc, much higher than those of water or low-pressure ice polymorphs (~1 g/cc). For instance, the high bulk density of Europa (Table 1) requires that the observed surface ice layer cannot extend very deep into its interior. Conversely, Tethys' extremely low bulk density suggests that it is almost entirely made of ice and thus any heating via radioactive decay will be very limited. For small bodies, a low density could be explained by high ice fraction or high porosity, but because pores close under pressure this effect is less important for the larger moons (e.g. Matson et al. 2009).

| | Distance ($R_p$) | Period (d) | Eccentricity | Bulk density, kg $m^{-3}$ | Mean radius, km | *a*, km | *b*, km | *c*, km |
|---|---|---|---|---|---|---|---|---|
| Europa | 9.4 | 3.55 | .0101 | 2989 | 1560.8 ± 0.3 | [1562.6] | [1560.3] | [1559.5] |
| Ganymede | 15.0 | 7.15 | .0015 | 1942 | 2634.1 ± 0.3 | [2635.2] | [2633.8] | [2633.4] |
| Callisto | 26.3 | 16.7 | .007 | 1834 | 2408.4 ± 0.3 | [2408.4] | [2408.3] | [2408.2] |
| Mimas | 3.08 | 0.942 | .0202 | 1149 | 198.2 ± 0.5 | 207.8 ± 0.5 | 196.7 ± 0.5 | 190.6 ± 0.3 |
| Enceladus | 3.95 | 1.37 | .0045 | 1609 | 252.1 ± 0.2 | 256.6 ± 0.3 | 251.4 ± 0.2 | 248.3 ± 0.2 |
| Tethys | 4.89 | 1.89 | .0000 | 985 | 531.0 ± 0.6 | 538.4 ± 0.3 | 528.3 ± 1.1 | 526.3 ± 0.6 |
| Dione | 6.26 | 2.74 | .0022 | 1478 | 561.4 ± 0.4 | 563.4 ± 0.6 | 561.3 ± 0.5 | 559.6 ± 0.4 |
| Rhea | 8.74 | 4.52 | .0010 | 1237 | 763.5 ± 0.6 | 765.0 ± 0.7 | 763.1 ± 0.6 | 762.4 ± 0.6 |
| Titan | 20.3 | 15.9 | .0292 | 1880 | 2574.8 | 2575.2 | 2574.7 | 2574.4 |
| Iapetus | 59.1 | 79.3 | .0283 | 1088 | 734.3 ± 2.8 | 745.7 ± 2.9 | | 712.1 ± 1.6 |
| Miranda | 4.95 | 1.41 | .0027 | 1201 ± 149 | 235.8 ± 0.7 | 240.4 ± 0.6 | 234.2 ± 0.9 | 232.9 ± 1.2 |
| Ariel | 7.30 | 2.52 | .0034 | 1665 ± 153 | 578.9 ± 0.6 | 581.1 ± 0.9 | 577.9 ± 0.6 | 577.7 ± 1.0 |
| Umbriel | 10.2 | 4.14 | .0050 | 1400 ± 184 | 584.7 ± 2.8 | - | | |
| Titania | 16.6 | 8.71 | .0022 | 1715 ± 56 | 788.9 ± 1.8 | - | | |
| Oberon | 22.3 | 13.5 | .0008 | 1630 ± 58 | 761.4 ± 2.6 | - | | |
| Triton | 14.1 | -5.88 | .0004 | 2061 | 1353.4 ± 0.9 | 1354.9 ± 0.9 | 1353.0 ± 0.9 | 1352.4 ± 0.9 |
| Pluto | - | - | - | 1854 ± 11 | 1188.3 ± 1.6 | - | | |
| Charon | 16.5 | 6.38 | <7e-5 | 1701 ± 33 | 606.0 ± 1.0 | - | | |

**Table 1**. Basic data for satellites. Distance is given in planetary radii ($R_p$), eccentricities are from Murray and Dermott (1999) except for Charon (Buie et al. 2012). Here *a,b,c* denote the three axes of the best-fit ellipsoidal shape. Sources of shape data are as follows: Europa – Nimmo et al. 2007, Ganymede & Callisto – Davies et al. 1998, Saturnian satellites except Titan – Thomas 2010, Titan – Hemingway et al. 2013 (Table S1), Uranian satellites – Thomas 1988, Triton – Thomas 2000, Pluto & Charon – Nimmo et al. 2017. Quantities in brackets were derived subject to the assumption of hydrostatic equilibrium.

*1.1.2 Induction.* An electrically-conductive body in a time-variable magnetic field will experience induction currents, which generate a secondary magnetic field. This is the basis of the successful detection of subsurface oceans on Europa, Ganymede and Callisto by the *Galileo* spacecraft (Zimmer et al. 2000, Kivelson et al. 2002). These satellites experience a time-dependent magnetic field because Jupiter's magnetic pole is offset from its rotation pole, so the field changes on Jupiter's orbital period. Europa and Callisto exhibited internal magnetic fields which varied with the external field - evidence for induction. The magnitude of the induced field places bounds on the depth and conductivity of the layer responsible; the most parsimonious explanation is a salty ocean. At Ganymede, in addition to the induced field a constant field was also detected, indicating that Ganymede (uniquely) has an active dynamo. Unfortunately, because Saturn's magnetic field is co-aligned with its rotation pole, this technique cannot be used by *Cassini*.

*1.1.3 Shape and Gravity*. If a planet has no long-term strength, its surface will conform to an equipotential determined by the body's rotation, tidal distortion and internal mass distribution (Murray & Dermott 1999). The dominant feature of the resulting shape is described by a spherical harmonic of degree $l$=2. Remarkably, this shape can be used via the so-called Darwin-Radau approximation (e.g. Stacey 1969) to deduce the mass distribution as described by the moment of inertia or MoI, denoted $C$. Equivalently, the $l$=2 gravity coefficients can likewise be used to deduce $C$. It is thus straightforward to measure $C$ for a strengthless body. The normalized MoI given by $C/MR^2$ is usually quoted, as it can be compared directly with that of a uniform body (for which $C/MR^2$=0.4).

Unfortunately, icy satellites are not obviously strengthless – for instance, Iapetus famously has a rotational bulge that "froze in" early in its history (Castillo-Rogez et al. 2007). One way of checking whether the shape or gravity conform to the strengthless ("hydrostatic") ideal is to measure the ratio of the two principal spherical harmonic coefficients, $C_{20}/C_{22}$. For a slowly-rotating hydrostatic body, this ratio is -10/3 (e.g. Tricarico 2014). Even if the shape and gravity are not hydrostatic, it is sometimes possible to separate out the hydrostatic and non-hydrostatic components, and establish a moment of inertia (e.g. Iess et al. 2014).

| | $J_2$ (x$10^6$) | $J_2/C_{22}$ | Inferred $C/MR^2$ | Reference |
|---|---|---|---|---|
| Europa | $435.5 \pm 8.2$ | [10/3] | [0.346] | Anderson et al. 1998 |
| Ganymede | $127.5 \pm 2.9$ | [10/3] | [0.312] | Anderson et al. 1996 |
| Callisto | $32.7 \pm 0.8$ | [10/3] | [0.355] | Anderson et al. 2001 |
| Enceladus | $5435.2 \pm 34.9$ | 3.51 | 0.335 | Iess et al. 2014 |
| Dione | $1454 \pm 16$ | 4.00 | 0.32-0.34 | Hemingway et al. 2016 |
| Rhea | $946.0 \pm 13.9$ | 3.91 | n/a | Tortora et al. 2016 |
| Titan (Sol 1a) | $33.6 \pm 0.3$ | 3.32 | 0.343 | Iess et al. 2012 |
| Titan (Sol 2) | $31.9 \pm 0.6$ | 3.20 | 0.344 | Iess et al. 2012 |

**Table 2**. Summary of gravity moments and inferred normalized moment of inertia for icy satellites. Here $J_2$=-$C_{20}$. Values in brackets indicate the ratio $J_2/C_{22}$ was fixed at 10/3. For Titan two independent solutions are given; also see Section 1.2.1.

*1.1.4 Geodesy*. There are several ways in which precise measurements of a satellite's orientation and surface position can be used to deduce its internal structure. One is to measure the amplitude of the satellite's diurnal tides (Wahr et al. 2006), either by tracking its surface deformation (yielding the so-called tidal $h_2$ Love number; Stacey 1969), or by measuring the resulting time-variable gravity (yielding the tidal $k_2$ Love number). A satellite lacking an ocean will typically exhibit lower tidal $h_2$ and $k_2$ than a satellite possessing an ocean; this is because the ocean decouples the deep interior (which is typically rigid and resistant to deformation) from the ice shell above (Moore & Schubert 2000).

A second approach is to look for librations, small periodic departures from a constant rotation rate (Tiscareno et al. 2009). An ellipsoidal rigid satellite in an eccentric orbit will experience periodic torques as it orbits its primary. These torques cause the satellite to spin up and spin down over the course of an orbit. The amplitude of the resulting librations depend on the (known) shape and orbital characteristics of the satellite, and also its moment of inertia. Thus, if the libration amplitude can be measured, the moment of inertia can be deduced. For a non-rigid satellite things become more complicated (Van Hoolst et al. 2013), but the basic principle remains the same.

A final approach is to measure the obliquity: the tilt of the satellite's rotation axis from the normal to its orbit plane. Both the orbit pole and the rotation pole will precess; dissipation in the satellite drives these two poles to remain coplanar with the mean orbit-pole location, a so-called Cassini state. In a similar way to librations, the obliquity depends on the known shape, the orbital inclination, and the moment of inertia. So if the obliquity can be measured, the moment of inertia can be deduced (Bills & Nimmo 2011). Note that, in contrast to the libration approach, an additional assumption (that the satellite is in a Cassini state) has to be made.

*1.1.5 Other approaches*. In some cases, information from other measurements can help to deduce interior structure. For instance, chemical measurements of the erupted materials at Enceladus helped determine its internal state (Section 1.2.4), and similar comments apply to measurements of Titan's atmosphere (Section 2.1.5). Direct measurements of the heat emitted at Enceladus's south pole (Section 2.1.2) have proven important in understanding its evolution. Telescopic observations of Europa suggest the presence of eruptive plumes there (Section 1.2.4) and Earth-based measurements of its obliquity may ultimately help determine its internal structure.

*1.2 What do we know?*

Having discussed the general techniques available, each satellite will now be described in turn. Figure 3 summarizes the inferred internal structures of the moons which have been subject to most scrutiny.

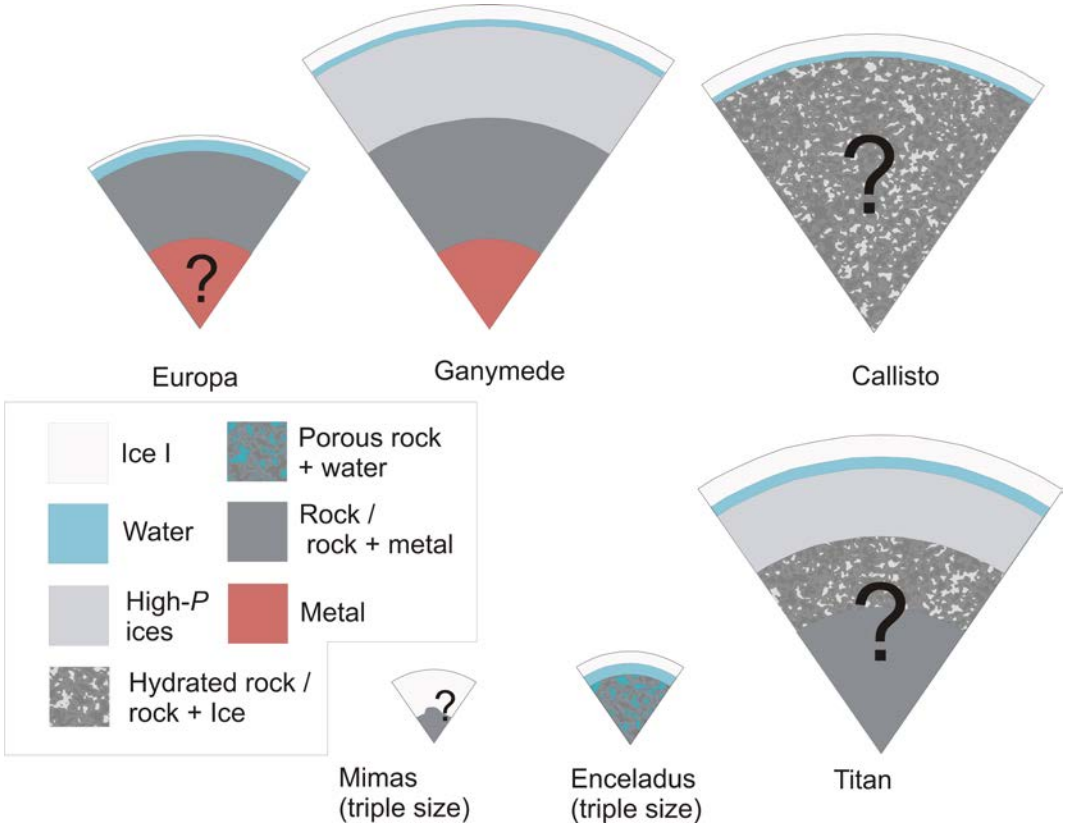


**Figure 3**. Inferred internal structures for selected moons. Question marks indicate regions of particular uncertainty. Note the lumpy core of Mimas, and that Mimas and Enceladus are plotted at three times the scale of the other moons.

*1.2.1 Titan*. Titan is a particularly complicated satellite, possessing as it does a thick atmosphere and liquid hydrocarbons at the surface. Because of its size, a subsurface ocean was thought likely even prior to the *Cassini* mission (e.g. Sohl et al. 2003).

*Cassini* measurements of Titan's obliquity (Stiles et al. 2008) provide the strongest evidence for a subsurface ocean. The obliquity of Titan is about three times larger than would be expected for a solid body; this large difference can be explained if the near-surface shell is decoupled from the interior by an ocean (Bills & Nimmo 2011, Baland et al. 2014). Alone of the icy satellites, Titan's tidal response has also been measured, yielding $k_2 \approx 0.4\text{-}0.7$ (Iess et al. 2012). This is higher than theoretically predicted values (Sohl et al. 2003), and suggests a highly deformable interior in addition to a shallow decoupling ocean. It also makes Titan's high eccentricity hard to explain (Section 3.1.2 below).

Early *Cassini* flybys showed that Titan's $l$=2 gravity was approximately hydrostatic (Iess et al. 2010), while its topography was not (Zebker et al. 2009). One likely explanation for this is that Titan experiences spatial variations in shell thickness, which are expected owing to spatial variations in tidal heating, and which result in a topography signal but no corresponding gravity signal (Nimmo & Bills 2010). The inferred shell thickness variations can be explained by mild tidal heating, but require that the ice shell be conductive rather than convective (Section 2.1.4). Absence of convection can be explained if the base of the shell is cold (e.g. because the ocean is $NH_3$-rich).

Taking Titan's degree-2 gravity to be hydrostatic, an MoI of 0.34 was inferred (Iess et al. 2012; Table 2). More recently, measurements of $l$=3 gravity and topography have been used to identify a non-hydrostatic component, likely resulting from a rigid near-surface layer ~100 km thick (Hemingway et al. 2013). Subtracting this non-hydrostatic component from the $l$=2 gravity and topography yields a normalized MoI which is model-dependent but might be as large as 0.36. Unfortunately, different interpretations of this number are possible (Tobie et al. 2014). It might mean that Titan really is incompletely differentiated, containing an intimate mixture of rock and ice; or it might mean that the silicates are hydrated and thus relatively low-density (Castillo-Rogez and Lunine 2010).

*1.2.2 Europa* Europa's bulk density indicates that it is mostly rock (Table 1). Because of the limited number of flybys, Europa's degree-two gravity coefficients are not *independently* determined (Table 2), so they cannot be used to test whether the body is hydrostatic (Anderson et al. 1998). Europa's shape is close to hydrostatic, but the uncertainties are large (Nimmo et al. 2007). Nonetheless, assuming hydrostatic behaviour, the gravity coefficients can be used to deduce a normalized MoI of 0.346, which is consistent with a thin (~100 km) $H_2O$ layer above the silicates.

The induction technique constitutes the strongest evidence for a subsurface ocean on Europa (Zimmer et al. 2000). The existing data only reveal the induction effect at a single period (Jupiter's rotation), so there is a tradeoff between the inferred conductor thickness and conductivity (Khurana et al. 2002). Nonetheless, a near-surface liquid water layer seems inescapable. In contrast, the thickness of the ice shell is currently quite uncertain. If Europa's silicate interior were Io-like, the tidal heat generated could maintain a shell only a few km thick (Greenberg et al. 2002). Lower tidal heating levels, probably concentrated in the ice shell, would result in a shell thickness of a few tens of km (Hussmann et al. 2002, Tobie et al. 2005). The largest impact features on Europa are more consistent with a thicker shell (Turtle & Pierazzo 2001, Schenk 2002), but most surface observations cannot distinguish between thin and thick

shells. Unlike Titan, the limited topographic data show no evidence for lateral shell thickness variations (Nimmo et al. 2007).

*1.2.3 Ganymede & Callisto* For Ganymede and Callisto, the same basic techniques were applied as at Europa. Induction revealed a subsurface ocean beneath Callisto (Zimmer et al. 2000), and a probable one at Ganymede (Kivelson et al. 2002), with interpretation at the latter being complicated by the presence of an internally-generated permanent field. As at Europa, the degree-two gravity coefficients could not be determined independently, so hydrostatic equilibrium had to be assumed. Under this assumption, Ganymede and Callisto have normalized MoI's of 0.312 and 0.355 (Anderson et al. 1996, Anderson et al. 2001). Interpretation of Ganymede's gravity is complicated by the presence of apparently local anomalies, similar to the "mascons" on the Moon (Palguta et al. 2006).

The MoI for Ganymede suggests a differentiated interior. This is consistent with its apparent ability to generate an internal magnetic field, implying a liquid iron core in which convection – driven by thermal or compositional buoyancy – is occurring (Hauck et al. 2006). For Callisto, the MoI value indicates an incompletely-differentiated body. This is surprising, because the inferred subsurface ocean implies some degree of differentiation. Although scenarios have been constructed in which these two apparently discrepant observations can be reconciled (Nagel et al. 2004), it may be that Callisto is cold enough that the hydrostatic assumption (and thus the derived MoI) are simply incorrect (McKinnon 1997).

*1.2.4 Enceladus* One of the biggest surprises of the *Cassini* mission was that tiny Enceladus was geologically active, venting water vapour and heat into space at its South Pole (Porco et al. 2006, Spencer et al. 2006). Measurements of the eruption products revealed salty ice grains (Postberg et al. 2011), immediately suggesting the presence of subsurface water. More recently, measurements of its anomalously large librations have proved that this subsurface water is a global ocean, not just a regional sea (Thomas et al. 2016).

The gravity and topography of Enceladus have been analyzed in a similar manner to Titan, decomposing them into hydrostatic and non-hydrostatic components and taking into account the effects of rapid rotation (Iess et al. 2014). By combining these results with the measured libration amplitude, a fairly precise picture has emerged (Hemingway et al., 2018), with an ice shell 20-30 km thick, overlying an ocean of comparable thickness and a low-density, presumably porous, silicate core with a radius of about 190 km. The ice shell is thinned to perhaps only a few km at the South Pole, presumably reflecting enhanced tidal heating there.

In situ measurements of the plume chemistry have been used to deduce high-temperature chemical reactions between the water and silicates (Hsu et al. 2015, Waite et al. 2017). Coupled with the low inferred density of the core, these observations suggest that water flushes through the core and is heated there, likely because the core is deformable and tidally-heated (Roberts 2015, Choblet et al. 2017).

*1.2.5 Other mid-sized Saturnian satellites* For the other Saturnian satellites, fewer constraints are available. Their bulk densities indicate varying rock:ice ratios (Table 1); Tethys in particular must be almost pure ice. Mimas, Enceladus, Iapetus, Titan and (arguably) Tethys all have degree-2 shapes which are not hydrostatic (Thomas et al. 2010, Nimmo et al. 2011); the other satellites are less distorted, so the uncertainties in their shapes are too large to be sure. Iapetus is distinguished by its large rotational bulge,

characteristic of a rotational period of ~16h and acquired long before it attained its present-day synchronous spin state (Castillo-Rogez et al. 2007).

Rhea's gravity is non-hydrostatic; combined with the uncertainties in its topography, this makes the interior structure hard to constrain (Tortora et al. 2016). By contrast, although Dione's gravity is also non-hydrostatic, an Enceladus-like analysis reveals a moment of inertia of ~0.33 (Hemingway et al. 2016) and the existence of a compensated ice shell, suggesting a subsurface ocean (Beuthe et al. 2016). No gravity moments are available for Mimas, Tethys or Iapetus.

As with Enceladus, librations have been measured at Mimas and have a slightly larger amplitude than would be expected for a rigid body of Mimas's shape (Tajeddine et al. 2014). There are two possible interpretations: either Mimas has a subsurface ocean, or it has subsurface mass anomalies that provide a larger torque than would be expected based on the surface shape. Given Mimas's small size and absence of geological activity, the latter explanation is much more likely, and might be due to a "lumpy" rocky core.

*1.2.6 Uranian satellites* Almost no information is available for these bodies. Although their shapes are approximately known (Thomas 1988), their masses (and thus bulk densities) are in some cases poorly constrained. Ariel, Miranda and Titania all show substantial surface deformation (Collins et al. 2009), most likely because of ancient tidal heating.

*1.2.7 Kuiper Belt Objects* Triton, with its retrograde orbit round Neptune, is generally thought to be a captured Kuiper Belt object (Agnor & Hamilton 2006). The capture and subsequent orbital circularization would have led to intense tidal heating and the expectation of complete differentiation (Goldreich et al. 1989). Triton's size and density make it a close cousin to Pluto. The *New Horizons* mission recently determined accurate shapes for both Pluto and Charon, revealing that Charon is about 10% less dense than Pluto (Nimmo et al. 2017). The bulk densities of all three objects suggest they consist of roughly two-thirds rock by mass (McKinnon et al. 2017).

Triton's ellipsoidal shape is slightly more distorted than would be expected for a fully-differentiated body (Thomas 2000), but the uncertainties are sufficiently large that this result may not be meaningful. There is no evidence for any rotational flattening of either Pluto or Charon (Nimmo et al. 2017), and no gravity data. Pluto is presumed to be differentiated, mainly because if it was undifferentiated, high pressure ice phase changes would have resulted in substantial contraction (McKinnon et al. 2017). Instead, the surface is peppered with extensional faults, consistent with a refreezing subsurface ocean (Moore et al. 2016).

## 2. Dynamics

Various dynamic processes are likely to have operated on the icy satellites and modified their surfaces. In some cases, surface observations can allow us to infer with confidence that a particular process has operated (e.g. impact craters, Section 2.2.3). In other cases, however, the surface observations can be ambiguous or controversial. For instance, surface fractures can arise through various different mechanisms, such as ice shell thickening, tidal stresses or polar wander. Images alone are generally insufficient to definitively identify "cryovolcanic" deposits (Section 2.1.5).

Below these processes are categorized as either internal or external. Internal processes on generic icy satellites are reviewed in McKinnon (1998), Matson et al. (2009) and Collins et al. (2010). For external

processes, impacts are covered by Melosh (1989) and tides and orbital evolution by Murray and Dermott (1999) and Peale (1999).

*2.1 Internal processes*

*2.1.1 Radioactive decay and long-term cooling* Decay of long-lived radiogenic elements (K,U,Th) can keep large satellites warm (Hussmann et al. 2006). For example, Pluto, which was never tidally-heated, could easily have maintained a subsurface ocean to the present-day purely by radioactive heating, as long as the ice shell above did not convect (Robuchon & Nimmo 2011). Similar conclusions apply to Titan, Callisto and Ganymede; Europa's ice shell is inferred to be so thin that some degree of tidal heating is required in addition (see below).

The present-day chondritic heating rate is about $3.4 \times 10^{-12}$ W/kg, with the rate being almost ten times higher at 4.5 Ga. For a typical satellite which is two-thirds rock by mass and has a radius of 200 km or 2000 km, the resulting present-day heat fluxes would be about 0.3 and 3 mW $m^{-2}$, respectively (neglecting any stored heat).

The slow decrease in radioactive heat means that subsurface oceans will tend to re-freeze over time. Because of the volume changes involved, near-surface extensional stresses will result (Nimmo 2004), unless high-P ice phases are present. This process probably explains the ubiquitous extensional tectonic features observed on mid-sized icy bodies – Dione, Rhea, Tethys, Ariel, Titania and Charon (Collins et al. 2009).

*2.1.2 Tidal heating* As mentioned above, a satellite experiences tidal heating at a rate given by (Wisdom 2008)

$$\dot{H} = \frac{3}{2}\frac{n^5 R^5}{G}\frac{k_2}{Q}\left[7e^2 + \sin^2\theta\right] \qquad (1)$$

where $n$ is the mean motion, $R$ is the satellite radius, $G$ is the gravitational constant, $e$ is the eccentricity and $\theta$ the satellite obliquity. The quantity $k_2$ is the tidal Love number (Section 1.1.4) and $Q$ is the dimensionless dissipation factor, where a high $Q$ implies a low dissipation and a small phase lag between the applied potential and the tidal response. The quantity $k_2/Q$ can also be written as Im($k_2$), where $k_2$ is now a complex number (Tobie et al. 2005). A perfectly elastic or perfectly inviscid satellite would have $k_2/Q=0$. A viscoelastic satellite will have a $k_2/Q$ that depends on the viscosity and rigidity of the individual layers and the forcing frequency (Tobie et al. 2005). The presence of an ocean increases $k_2$ (Moore & Schubert 2000) and also usually results in a larger $k_2/Q$ (more dissipation).

For an isolated satellite, the torques associated with tidal heating tend to circularize the orbit (Murray and Dermott 1999). As a result, the tidal heating rate decreases. Thus, one would expect an isolated satellite to be in a circular orbit experiencing no tidal heating. Triton comes close to fulfilling this expectation, but other bodies (Europa, Enceladus etc.) are in orbital resonances which continually pump up the eccentricity and counteract the effect of circularization. A satellite with a larger inclination will typically have a higher obliquity (Section 1.1.4), so that inclination-type resonances can also lead to enhanced tidal heating. These issues are discussed in more detail below (Section 3.1.2).

The local rate of tidal heating depends on the local material properties. Ice near its melting point has a viscoelastic response timescale comparable to satellite orbital periods, which results in a large $k_2/Q$ and high tidal heating (Moore & Schubert 2000). Solid rocky cores have much longer response timescales, resulting in much less heating. Tidal heating also varies laterally (Beuthe 2013); in thin ice shells, the heating rate is a factor of ~2 higher at the poles than at the equator and can result in shell thickness variations (Ojakangas & Stevenson 1989).

Subsurface oceans also respond to tides, and could in principle dissipate heat (Tyler 2008). The physics differs to that of solid regions, because oceans are almost inviscid and turbulent. Obliquity tides turn out to be more effective at driving ocean tidal heating than eccentricity tides, but it now seems that the total power dissipated in subsurface oceans is most likely too small to matter, except perhaps for Triton (Chen et al. 2014). The presence of a rigid shell on top of the ocean further reduces the dissipated power (Beuthe 2016).

Tidal heating is most evident at Enceladus, where the 5-15 GW heat being emitted at the South Pole (Spencer et al. 2018) must ultimately come from tides. Although it was originally presumed that the heat was being generated in the ice shell, the shell is now thought to be so thin (Section 1.2.4) that a deformable core seems a more likely location of the heat (Roberts 2015). This is also consistent with presumed products of hydrothermal circulation detected in the erupted materials (Choblet et al. 2017). The asymmetry between the north and south poles of Enceladus is hard to explain, because tidal heating is symmetric about the equator.

The existence of a relatively thin ice shell on Europa (Section 1.2.2) is also explicable by tidal heating. Ganymede and Callisto are not significantly tidally-heated at the present day, owing to their greater distances from Jupiter. Titan is probably mildly tidally-heated, with lateral heating variations likely responsible for inferred shell thickness variations (Section 1.2.1). How Titan's high eccentricity can be reconciled with its high measured $k_2$ (Section 1.2.1) represents an open question: presumably Titan's $Q$ is high (low dissipation), though how this arises is uncertain.

Triton was almost certainly violently tidally-heated in the past (Section 1.2.7); it doesn't experience significant eccentricity tides at present, but might experience heating from its predicted obliquity (Chen et al. 2014). Charon may have been tidally-heated previously (Rhoden et al. 2015), but its orbit is currently circular (Buie et al. 2012). Further discussion of other possible ancient tidal heating episodes will be deferred to Section 3.1.2.

*2.1.3 Flexure & relaxation* The viscosity of ice is expected to decrease with depth (Section 1). This rheology structure can be approximately described by assuming an elastic layer with a thickness defined by a particular isotherm. Thus, if the thickness of the elastic layer can be determined, the temperature structure at the time of loading, and thus the heat flux, can be approximately inferred (e.g. Nimmo et al. 2002). This is very useful for inferring thermal histories (see Section 3.1). In practice, different regions of a satellite sometimes show differing elastic thicknesses: this might either be because of spatial variations in heat flux, or because the loads were emplaced at different times.

Topography derived from altimetry or (more usually) stereo imaging is available for most of the icy satellites. Using topography, it is often possible to identify individual loads and the resulting surface deformation. At its simplest, the characteristic wavelength of the response, known as the flexural

parameter $\alpha$, can be inferred from the topography and related directly to the thickness of the deforming elastic layer, $T_e$:

$$\alpha = \left( \frac{ET_e^3}{3(1-\nu^2)g\Delta\rho} \right)^{1/4} \quad (2)$$

where here $E$ is the Young's modulus of ice (nominally 9 GPa), $\nu$ is the Poisson's ratio, $g$ is the surface acceleration and $\Delta\rho$ is the density contrast between the material beneath the shell and the overlying material (in this case vacuum) (Turcotte and Schubert 2002)

Roughly speaking, the transition from elastic to viscous behaviour is expected to occur at about half the melting temperature, or about 130 K. At these temperatures, ice thermal conductivity is about 5 $Wm^{-1}K^{-1}$ (Ross & Kargel 1998) so for Enceladus (surface temperature 80 K), a 1 km elastic thickness would imply a heat flux of roughly 250 $mWm^{-2}$, comparable to what is observed at the South Pole.

Table 3 gives a selection of inferred elastic thicknesses for different bodies. For Europa, a wide range of $T_e$ values has been obtained, depending on the feature examined (Billings & Kattenhorn 2005). This might be due to high spatial variability in heat flux; for instance, the ubiquitous double ridges (which give low $T_e$ values) might be being heated in some fashion (Dombard et al. 2013). Table 3 shows typical $T_e$ values of a few km, compared with the tens or hundreds of km obtained for silicate bodies. The implied heat fluxes are tens to hundreds of $mWm^{-2}$, much higher than the anticipated present-day radiogenic heat flux (see above).

| **Body** | **$T_e$ (km)** | **Reference** | **Body** | **$T_e$ (km)** | **Reference** |
|---|---|---|---|---|---|
| Enceladus | 0.3 | Giese et al. 2008 | Dione | 2.5-4.5 | Hammond et al. 2013 |
| Ganymede (bright, young) | 0.9-1.7 | Nimmo et al. 2002 | Ariel | 3.8-4.4 | Peterson et al. 2015 |
| Miranda | 2 | Pappalardo et al. 1997 | Tethys | 5-7 | Giese et al. 2007 |
| | | | Iapetus | 50-100* | Giese et al. 2008 |

**Table 3**. A selection of flexurally-derived elastic thicknesses for icy bodies. *The Iapetus value is an over-estimate because the authors ignored the effect of membrane stresses.

An alternative approach to inferring ancient heat fluxes is to look for anomalously shallow (relaxed) impact basins. An impact feature exerts stresses on the ice beneath; if the ice is sufficiently warm, it will flow in response to these stresses and gradually erase the basin (Melosh 1989). The rate of relaxation depends on the crater dimensions and the subsurface temperature gradient. On some parts of Enceladus and Ganymede, heat fluxes were sufficiently high that even quite small craters are relaxed (Bland et al. 2012, 2017). Impact basins on Dione, Rhea and Tethys are shallower than comparable basins on Iapetus, implying heat fluxes of at least a few tens of $mWm^{-2}$ operating over at least a few Myr (White et al. 2013, 2017). These high inferred heat fluxes are generally consistent with independent estimates obtained from flexural studies (see above) and are almost certainly caused by tidal heating.

*2.1.4 Convection* A thin ice shell will remove heat generated in the interior by conduction. The resulting temperature profile is not linear, however, because the thermal conductivity of ice goes as roughly $1/T$ (Ross & Kargel 1998). If the ice shell is thick enough, heat will instead by transferred by convection. Convection is important for three reasons. First, it increases the rate of cooling, which means that it is

harder to sustain a subsurface ocean. Second, it alters the viscosity structure of the ice shell, and thus the amount and distribution of tidal heating. And, third, it can give rise to features visible at the surface.

The viscosity of ice near its melting point is probably around $10^{14}$ Pa s, depending on grain size (Goldsby & Kohlstedt 2001). As a result, even moderately thin ice shells are likely to undergo convection. Whether ice shell convection occurs is determined by the Rayleigh number *Ra*, defined as (Solomatov 1995):

$$Ra = \frac{\rho g \alpha \Delta T d^3}{\kappa \eta_b} \quad (3)$$

where $\rho$ is the density, $g$ the gravity, $\alpha$ the thermal expansivity, $\Delta T$ the temperature contrast between top and bottom of the ice shell, $d$ is the shell thickness, $\kappa$ the thermal diffusivity and $\eta_b$ the viscosity at the base of the ice shell, temperature $T_b$. In reality, this viscosity is probably dependent on the stress applied, in which case equation (3) needs modification (see Barr et al. 2004, Solomatov 1995).

For convection to occur, *Ra* must exceed a critical Rayleigh number, $Ra_{cr}$. For strongly temperature-dependent materials like ice, the critical Rayleigh number is typically ~$10^7$ and is given by

$$Ra_{cr} = 20.9(x\gamma\Delta T)^4 \quad (4)$$

Here $x$ is a geometrical factor (see below) and $\gamma$ describes the sensitivity of the viscosity to temperature:

$$\eta(T) = \eta_b \exp(-\gamma [T-T_b]) \quad (5)$$

and is related to the activation energy $E_a$ by $\gamma = E_a/R_g T_b^2$, where $R_g$ is the gas constant. The geometrical factor $x$ arises from the fact that it is harder to initiate convection in a spherical shell than a flat plate. For the Cartesian (flat-plate) case $x$=1 and for an Enceladus-like situation, $x \approx 2$ (Appendix B of Robuchon & Nimmo 2011). Application of these equations to the case of Europa suggests that an ice shell thicker than about 15 km is expected to undergo convection.

Deducing whether convection is occurring from surface observations is challenging. One problem is that near-surface ice is so cold that even if convection occurs, a “stagnant lid” which remains undeformed is expected (Solomatov 1995). This may not be true in practice – real geological materials typically have a “yield strength” beyond which convection can cause the surface layer to deform (e.g. Tackley 2000). It has been suggested that some landforms on Enceladus and Ganymede may be the resulting of convection-driven yielding (Showman & Han 2005, Barr & Hammond 2015), but this is uncertain. Small-scale “domes” and “pits” on Europa might be the result of convection, but are more plausibly caused by the intrusion of liquid water (Manga and Michaut 2017). The most convincing example of convection in the outer solar system is the nitrogen plains of Sputnik Planitia, Pluto, which display a cellular pattern almost certainly indicative of convection (McKinnon et al. 2016). The strange “cantaloupe terrain” of Triton might be the result of convection, but with the motion driven by compositional rather than thermal buoyancy (Schenk and Jackson 1993). The enigmatic coronae at Miranda may have arisen in a similar fashion (Pappalardo et al. 1997).

Because convection reduces the viscosity relative to a conductive situation, it tends to enhance tidal heating, which can further enhance the convective motion and thus produce a feedback cycle and

(potentially) local melting (Sotin et al. 2002, Behounkova et al. 2012). The high-pressure ice layers in Titan, Callisto and Ganymede likely undergo convection (McKinnon 1998) and are subject to similar feedbacks, but have not been much studied.

*2.1.5 Cryovolcanism* Cryovolcanism – the eruption of low-temperature liquids or gases to the surface – is a somewhat controversial subject. Explosive cryovolcanic eruptions are now known for sure at Enceladus, with some confidence at Europa, and possibly at Triton. Effusive eruptions of low-viscosity liquids, however, have never been caught in action but only inferred, based mainly on imaging.

Cryovolcanism suffers from the theoretical problem that, unlike silicate volcanism, the melt is denser than the solid. This makes it hard for eruptions to happen, although many solutions have been proposed, notably exsolution of gaseous species (Crawford & Stevenson 1988), ocean compression (Manga & Wang 2007), topographic forcing (Showman et al. 2004) or "tidal pumping" (Greenberg et al. 2002).

The only cast-iron example of cryovolcanism is at Enceladus (Porco et al. 2006). What appears to be happening is that water-filled fractures are periodically exposed to vacuum, boiling the water off into space (Spencer et al. 2018). The fractures must open and close in response to diurnal tidal stresses (Hurford et al. 2007), because the resulting eruption plume is seen to be modulated on a tidal period (Hedman et al. 2013, Nimmo et al. 2014).

Two different Earth-based imaging approaches have captured apparent eruptive plumes at Europa (Roth et al. 2014, Sparks et al. 2017). If real, these are larger than their counterparts at Enceladus, but do not appear to exhibit the same kind of diurnal modulation. Eruptive geysers were imaged at Triton, but there is still debate as to whether these are driven by surface heating, or subsurface processes (Kirk et al. 1995).

Emplacement of low-viscosity cryovolcanic surface flows has been suggested for various icy satellites. But these claims should be viewed cautiously: Moore & Pappalardo (2011) document how hard it is to definitively identify cryovolcanic deposits, and how past identification of such features has been proven incorrect when higher-resolution images were returned.

The most contentious case is Titan. One reason that cryovolcanism is favoured there is that Titan's atmosphere suffers from gradual photochemical destruction of $CH_4$, on a timescale of tens of Myr. The surface hydrocarbons are insufficient to replenish what is lost, so some deeper $CH_4$ source must be invoked. Similarly, the $^{40}Ar$ detected in the atmosphere must ultimately be produced by $^{40}K$ decay in silicates. Both these observations suggest transport from the interior to the surface (Tobie et al. 2014). Whether this transport has to involve cryvolcanism of the kind invoked based on images is an open question. A recent summary of potential cryovolcanic features on Titan may be found in Lopes et al. (2013).

Low-viscosity cryolavas may also have been responsible for some landforms on Triton (Croft et al. 1995), Miranda & Ariel (Schenk 1991), Ganymede (Schenk et al. 2001) and Europa (Fagents 2003), although in all cases the evidence is somewhat equivocal. Higher-viscosity flows might be responsible for the smooth plains of Charon and the two large, enigmatic mounds imaged at Pluto (Moore et al. 2016). Cryovolcanic intrusions are even harder to identify, although Manga and Michaut (2017) make a strong case that the pits, spots and domes seen on Europa are likely of intrusive origin.

*2.1.6 True polar wander & non-synchronous rotation* The diurnal component of a satellite's tidal bulge will produce torques which, in the absence of other torques, will cause the satellite to rotate slightly faster than synchronous (Greenberg & Weidenschilling 1984). In practice, these torques are likely to be counteracted by tidal torques on permanent mass anomalies (e.g. the Ganymede mascons) or the effects of an overlying elastic shell (Goldreich and Mitchell 2010), but the uncertainties are large. Thus, non-synchronous rotation (NSR) of a satellite is theoretically permitted. One important consequence of NSR is that it can result in much larger stresses than those generated by diurnal tides (Collins et al. 2009).

There is very little direct evidence for NSR. A radar detection of NSR at Titan was claimed (Lorenz et al. 2008) but this turned out to be a software error. Comparisons of images of Europa taken at different epochs have only succeeded in placing upper bounds on the NSR rate (Hoppa et al. 1999a). Attempts to use geological features to infer the presence or absence of NSR have not been successful (Rhoden & Hurford 2013). One possible line of evidence for NSR is the longitudinal distribution of impact craters, discussed in Section 2.2.3.

If mass is added to (or subtracted from) a satellite, tidal and rotational torques will cause the satellite surface to move relative to its fixed rotation pole, a situation referred to as True Polar Wander (TPW). The amount of TPW which occurs depends on how large the mass change is compared with the frozen-in tidal and rotational bulges, which oppose any motion (Nimmo & Matsuyama 2007). The importance of TPW is that, like NSR, it generates a global pattern of stresses which can be compared with the observed distribution of tectonic features (Matsuyama & Nimmo 2008).

It has been shown that, at least at Europa, shell thickness variations caused by tidal heating (Section 2.1.2) could result in TPW (Ojakangas & Stevenson 1989). Remarkably, Europa exhibits a global network of troughs with orientations which agree fairly well with the predicted TPW (Schenk et al. 2008). The active region of Enceladus may be at the South Pole because of TPW (Nimmo & Pappalardo 2006), with the presumed warm ice acting as a negative mass anomaly and driving polewards motion. Something similar may have happened to the coronae at Miranda. Conversely, at Pluto the deep basin of Sputnik Planitia may have moved towards the equator, driven by nitrogen deposition in the basin (Nimmo et al. 2016, Keane et al. 2016). Large impact basins on other satellites may also have caused TPW episodes (Nimmo & Matsuyama 2007), though direct evidence is lacking.

*2.2 External*

As noted above, the main source of energy driving icy satellite dynamics is tides. As a result, there is a strong coupling between internal dynamics and how a satellite orbit evolves. Below both short-period (days-years) and long-period (~Myr) orbital effects are discussed; further details can be found in Section 3.1.2 below and in Murray & Dermott (1999). The effects of impacts, which not only leave visible traces but can potentially affect orbital evolution as well, are also reviewed.

*2.2.1 Short Period Orbital Effects* As noted above, diurnal tides result in heating and generate stresses which may lead to formation of surface features. A possible example of the latter phenomenon is the so-called "cycloids" on Europa (Hoppa et al. 1999b). Diurnal tides also modulate eruptive behaviour on Enceladus (Section 2.1.5); longer-period variations in orbital characteristics may be responsible for the decadal modulation observed there (Ingersoll & Ewald 2017).

*2.2.2 Long Period Orbital Effects* The evolution of satellite orbits on long timescales is dominated by the competing effects of dissipation in the primary, and dissipation in the satellite. Dissipation in an isolated satellite drives the eccentricity towards zero, truncating tidal heating. By contrast, dissipation in the primary results in torques which push the satellite outwards and spin the primary down. Because the torques are a strong function of semi-major axis, the result is usually that inner satellites migrate outwards faster (Figure 4). This is important, because it may cause a pair of satellites to pass through an orbital resonance, in which the ratio of their periods is a simple integer ratio (2:1, 3:2 etc.). If captured into a resonance, the mutual orbital perturbations cause the satellite eccentricities (or inclinations) to grow and thus boost tidal heating (with the ultimate energy source being the primary's rotation). The reason that tidal heating is so apparently common is because of the existence of ancient or present-day resonances. More detailed discussion of the consequences is deferred to Section 3 below.

*2.2.3 Impacts and disruption* Outer solar system bodies suffer bombardment from comets, exemplified by the collision of Shoemaker-Levy 9 with Jupiter. These impacts are useful to two main reasons: first, they provide a way of estimating surface age; and second, impacts can probe the subsurface structure.

An ancient surface will have experienced more impacts than a younger surface, so relative age-dating is fairly straightforward. Obtaining an absolute surface age requires a knowledge of the impact flux, and how it has changed over time, which is very far from straightforward. Zahnle et al. (2003) provide a comprehensive discussion of the issues involved, and estimates of the surface ages of various outer solar system bodies (all of which are subject to large errors). Some lightly-cratered surfaces, such as Europa, Triton and the South Pole of Enceladus, are probably less than 100 Myr old. Ganymede is divided into dark terrain (which is about as old as the solar system), and bright terrain which is perhaps ~1-2 Gyr old. Iapetus is heavily cratered and in particular has an anomalously large number of big impact basins, suggesting a bombardment history that is qualitatively different to that of the inner moons (Dones et al. 2009). Titan displays few impact craters, because of erosion and sediment deposition.

Zahnle et al. (2003) assume that the impactor population is dominated by heliocentric comets. A consequence of such impacts is that the leading side of a satellite should be more heavily cratered than its trailing side (Zahnle et al. 2001). Although there may be subtle leading-trailing asymmetries on some bodies (Hirata 2016), the size of the observed effect is much smaller than predicted. There are two possible explanations. Either the satellites have experienced NSR (or some other reorientation), smearing out the asymmetry. Or the population of impactors has a strong planetocentric component, since these bodies would not preferentially hit the leading hemisphere.

The Zahnle et al. (2003) age estimates assume a steadily declining impactor population. But at least on the Moon, there is some evidence for an impact "spike" at 3.9 Gyr B.P. (Morbidelli et al. 2012). Dynamical explanations for this spike typically result in a large flux of impactors throughout the solar system. For the inner Saturnian moons, this kind of impact would have had a catastrophic effect, breaking them apart many times over (Charnoz et al. 2009, Movshovitz et al. 2015). The moons would have subsequently re-accreted rapidly (Marzari et al. 1998), with their internal structures scrambled and subsequent crater production dominated by planetocentric impactors. A more recent, catastrophic collision has been suggested as a potential explanation of the Saturnian system architecture (Sekine & Genda 2012, Asphaug & Reufer 2013). And Charon may have formed via a giant impact with Pluto (Canup 2005), in a manner similar to the formation of the Earth's moon.

Impact craters on icy satellites undergo a regular progression in morphology as they increase in size. Small craters are bowl-shaped, larger craters develop a central peak, and the transition diameter depends on gravity (Melosh 1989). Crater appearance can in principle be related to subsurface structure: for instance, the multi-ringed basins on Europa, Ganymede and Callisto probably indicate a reduction in strength with depth (Melosh 1989), and the shallowness of large Europan impact structures may be a result of a thin ice shell underlain by an ocean (Schenk 2002).

## 3. Evolution

In terms of satellite evolution, we are interested in how they formed, and how they subsequently evolved. The latter will be discussed first, because it is somewhat better constrained by observations, and is closely related to orbital dynamics as discussed above. Papers reviewing these topics include Canup & Ward (2009), Tobie et al. (2014), Castillo et al. (2018) and Nimmo et al. (2018).

### *3.1 How did they subsequently evolve?*

Satellite evolution – and especially the development and survival of subsurface oceans – is largely governed by energetics, though chemistry (e.g. ammonia) can also play a role. The largest sources of energy (by far) are radioactive decay and tidal heating.

*3.1.1 Radioactive decay* Radiogenic heating can occur via short-lived or long-lived nuclides. The most important short-lived nuclide is $^{26}$Al, which has a half-life of only 0.7 Myr. If satellite accretion happened before this nuclide was exhausted, *all* regular satellites should have differentiated. So if Titan and Callisto are not differentiated, this places a limit on how fast they could have accreted (see below). The role of long-lived nuclides is discussed in Section 2.1.1.

At least for the Saturnian satellites and beyond, ammonia may have played an important role in sustaining subsurface oceans (Hussmann et al. 2006). Because it is excluded from ice, $NH_3$ concentrations in the remaining liquid increase as freezing proceeds, and so the freezing temperature drops. This slows the freezing rate. Perhaps even more important, the decreasing temperature at the base of the ice shell increases the viscosity there. As a result, the Rayleigh number (eq. 3) drops, and at some point convection shuts off. Since conduction is less efficient at cooling than convection, this effect further prolongs the ocean lifetime.

*3.1.2 Tidal heating and orbital evolution* For most satellites, especially small ones, tidal heating is dominant. Its effects are tricky to assess, however, because it depends on the internal structure of the satellite, and the evolution of the satellites' orbits. As a result, unlike radiogenic heating, tidal heating can be non-monotonic.

Tidal heating normally arises when satellites are trapped in a resonance (Section 2.2.2). At present, Enceladus and Dione are in a 2:1 eccentricity resonance, Io, Europa and Ganymede are in a 1:2:4 eccentricity resonance (the Laplace resonance), and Mimas and Tethys are in a 2:1 inclination-type resonance. These resonances probably arose because of the outwards drift of the satellites driven by dissipation in the primary (see 3.2.2 below). This outwards drift also means that other resonances may have existed in the past. Figure 4a shows a model of the outwards evolution of the Saturnian satellites, highlighting some of the possible paleo-resonances which may have occurred. Similar diagrams can be constructed for the Jovian and Uranian systems.

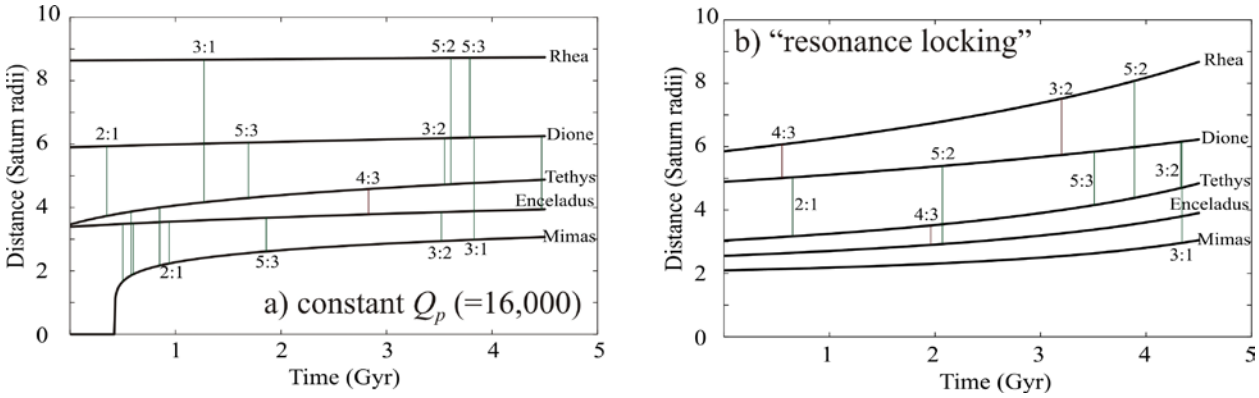


**Figure 4**. Outwards evolution of Saturnian satellites. a) Evolution driven by dissipation in Saturn with $Q_p$ set to a constant value. The same plot applies to any constant $Q_p$, with the timescale scaled by $Q_p$/16000. Vertical lines denote selected resonances with orbits on converging (green) and diverging (red) trajectories. b) As for a), but using the "resonance-locking" approach of Fuller et al. (2016) in which the effective $Q_p$ is higher for satellites with shorter periods (see text). Modified from Nimmo et al. (2018).

The details of whether capture into resonance occurs, and whether the resonance persists, are complicated and depend on the satellites' internal structures ($k_2/Q$). But in many cases there is observational evidence suggesting that some paleo-resonance must have occurred. One good example is Ganymede, which appears to have undergone a dramatic heating episode mid-way in its history, creating the tectonically-deformed bright terrain (Section 2.2.3). The leading explanation for this event is that the satellite was tidally heated when it was trapped in a "Laplace-like" resonance, prior to attaining its present-day orbital configuration (Showman & Malhotra1997). Similarly, the high ancient heat flux inferred at Tethys may have been due to passage through a 3:2 resonance with Dione (Chen & Nimmo 2008), and something similar may also have happened at Ariel (Peterson et al. 2015). The Uranian satellites almost certainly experienced paleo-resonances, but there are no resonances at the present day. The reason appears to be that the resonance widths are sufficiently large that they overlap, and are therefore unstable (Dermott et al. 1988). Although some paleo-resonances break spontaneously when eccentricities grow large enough, others are sufficiently stable that escaping from them is very difficult (e.g. Meyer & Wisdom 2008, Cuk et al. 2016). In some cases impacts may have been responsible for breaking such resonances (Zhang & Nimmo 2012).

As if all this were not complicated enough, there are two additional effects which require discussion.

*Equilibrium & Feedbacks*. In a resonance, dissipation in the primary increases $e$, while dissipation in the satellite decreases it. As a result, there is a competition between these two effects. One possible consequence is that the eccentricity evolves towards an equilibrium value. In this case, the rate of tidal heating in the satellite is *independent* of the satellite $k_2/Q$ (Meyer & Wisdom 2007) and depends only on the rate of dissipation in the primary (see below).

An alternative is that the eccentricities of the satellites exhibit periodic behaviour. This can happen because dissipation in the satellite depends on its interior structure, as described by $k_2/Q$. Tidal heating changes the satellite's internal temperature, modifying $k_2/Q$; if this changes, so too will the rate of change of eccentricity. There is thus a feedback loop between eccentricity and $k_2/Q$, and if the characteristic evolution timescales of these two quantities are similar, periodic behaviour can arise (Ojakangas &

Stevenson 1986, Hussmann & Spohn 2004). Periodic behaviour is quite likely for Europa-Io, and possible for Enceladus-Dione (Shoji et al. 2014).

*Dissipation in the Primary*. Dissipation in the primary is parameterized by the quantity $Q_p$, where the phase lag between the perturbing potential and the primary's response is ~1/2$Q_p$. Thus, for example, the equilibrium tidal heating rate for Enceladus is 1.1 GW (18,000/$Q_p$) (Meyer & Wisdom 2007), so that a more dissipative Saturn has a lower $Q_p$ and generates a higher heating rate. Assuming that Enceladus's current heat output of 5-15 GW is due to current tidal heating, the implied $Q_p$ for Saturn is 1300-4000. Recent astrometric studies of the long-term orbital evolution of the Saturnian satellites (Lainey et al. 2017) suggest that $Q_p$ at the Enceladus period is indeed about 1300, and that at Rhea's period it is even less.

These $Q_p$ values produce an immediate problem. Outwards satellite migration happens at a rate proportional to $Q_p$, so if $Q_p$ for Saturn really is 1300, then Figure 4a implies that Mimas is less than 0.5 Gyr old! Although Mimas is heavily cratered, this suggestion is not as outlandish as it seems at first. If the inner moons were broken apart by some recent catastrophic event, the appearance of Mimas could be reconciled with a young age (Section 2.2.3).

However, there is an alternative explanation which is perhaps more promising. Figure 4a is calculated assuming that the $Q_p$ of Saturn is constant. But the astrometric results themselves show that $Q_p$ is different at different periods. Recently, Fuller et al. (2016) have proposed that the effective $Q_p$ of Saturn is strongly frequency-dependent, and is ultimately controlled by Saturn's evolution timescale. This is termed the "resonance locking" scenario, and results in a $Q_p$ that is higher (less dissipative) at shorter periods. The effect of this scenario is shown in Fig 4b. By construction, it matches the astrometrically-derived present-day $Q_p$ values, but it results in much less outwards satellite migration. This approach can thus explain the present-day heat output of Enceladus without requiring Mimas to be young.

For the Jupiter system, the effective $Q_p$ is larger than for Saturn (Lainey et al. 2009), so outwards evolution of the Galilean satellites is less rapid. Note, however, that their detailed orbital trajectories will still differ from those obtained assuming a constant $Q_p$.

*3.2 How did they form in the first place?*

*3.2.1 Accretion scenarios* Broadly speaking, there are two scenarios for how the icy satellites might have formed. The first scenario assumes that all the mass which ultimately went into the satellites was present in orbit round the primary at the same time. This is identical to the assumption made for planet formation. But because satellite orbital timescales are days rather than years, accretion is expected to have proceeded much faster than for planets, taking perhaps $10^2$-$10^5$ years to complete (Squyres et al. 1988, Mosqueira & Estrada 2003). This scenario is hard to achieve unless the proto-satellite disk has a very low viscosity, which seems unlikely (Ward and Canup 2010). The second scenario assumes that mass was fed in gradually, so that the solid surface density was never as high as in the first case (Canup & Ward 2002). As a result, satellite accretion takes longer. If pairs of satellites are captured into mean motion resonances, they may be prevented from colliding with each other (Ogihara & Ida 2012) and growth will thus stall.

In both cases, satellite accretion probably takes place in a gaseous background. As a result, proto-satellite material experiences an inwards drift, potentially resulting in some satellites being absorbed into the

primary (Canup & Ward 2006). The presence of gas can also strongly affect the behaviour of cm-scale particles ("pebbles"). If a larger proto-satellite is already present, the gas drag experienced by the pebbles can cause them to be very efficiently captured by the proto-satellite, resulting in rapid growth (Ronnet et al. 2017). This style of "pebble accretion" is the leading explanation for why wide binaries are so common in the Kuiper Belt (Nesvorny et al. 2010).

*3.2.2 Observational Constraints* Unfortunately, there are limited observational constraints available to distinguish between the competing scenarios. One intriguing constraint is the regular progression in density and bulk composition in the Jovian system - from Io (100% rock) to Europa (~90% rock) to Ganymede and Callisto (~65% rock) – and its absence in the Saturnian and Uranian systems. A second constraint is that Titan and (perhaps) Callisto may only be incompletely differentiated (Sections 1.2.1, 1.2.3). A third comes from chemistry: the ratio of noble gases to $N_2$ in Titan's atmosphere suggests that the volatiles were not acquired directly from the proto-Saturn nebula (Tobie et al. 2014). But why Titan, and not Ganymede and Callisto, retained a thick atmosphere is currently unknown (Griffith & Zahnle 1995).

Collisions deliver mass and energy to the target. If the energy is delivered in small objects, only the near-surface is heated, and that heat can be radiated away. If the energy is deeply-buried, however, radiative cooling is ineffective. The internal temperature during accretion thus depends on the size-distribution of impacting material, and the rate at which mass is delivered (Squyres et al. 1988). Crucially, if a satellite gets too hot, the ice will melt and differentiation will take place. Thus, if Titan and Callisto really are only partially differentiated, constraints can be placed on how they formed (Barr et al. 2010, Barr & Canup 2010). Unfortunately, given the uncertainties associated with the internal structures of both bodies, it is hard to draw definitive conclusions.

In principle, the regular density progression of the Galilean satellites could be due to an initial temperature (and thus compositional) gradient in the proto-satellite disk, or later preferential ice loss in the inner regions driven by impacts or tidal heating (both of which are distance-dependent). As discussed in Dwyer et al. (2013), efficient radial mixing destroys any initial compositional gradient, while impacts do not appear capable of causing the required effect. While tidal heating is a possible answer, the massive tidal heating inferred for Triton evidently failed to remove the ice present on that moon.

So the cause of the radial density gradient for the Galilean satellites is obscure. Moreover, neither the Saturnian nor the Uranian moons show any such consistent pattern (Table 1). At least for the Saturnian case, the scattered densities have been attributed to the effects of a catastrophic collision (Sekine & Genda 2012, Asphaug & Reufer 2013), but direct evidence of such an event is lacking.

*3.2.3 When did they form?* It is usually assumed that the satellites formed at the same time as their primaries did. Triton and Charon are possible exceptions – Triton's capture could have occurred later, and if Charon formed in a giant impact it too may be a relative late-comer. However, it is possible to create scenarios in which other satellites are younger. For instance, Canup (2010) and Charnoz et al. (2011) show that if a dense ring of material is formed (e.g. by a pre-existing moon being pulled apart by tides), that ring will spread outwards. Once it spreads beyond the "Roche limit" (where tidal disruption occurs), the ring particles will coalesce to form proto-satellites. Torques from the ring will evolve these proto-satellites further outwards, possibly causing collisions and further growth. Formation of the Saturnian

satellites within the last 1 Gyr has also been suggested on dynamical grounds (Cuk et al. 2016), but in this scenario a constant $Q_p$ for Saturn was assumed, which is probably not correct (Section 3.1.2).

At present, there seems little prospect of distinguishing between "old" and "young" satellite scenarios. Although impact craters are used to date surfaces, to do so requires a model impact flux – and that will change drastically depending on which scenario is adopted. Other measures of absolute age are currently lacking, largely because samples of outer satellite materials are not available for analysis.

## 4. Summary and Outstanding Questions

Icy satellite dynamics is a hard problem, partly because of the absence of samples compared with silicate bodies, and partly because thermal-orbital feedbacks make their histories intrinsically more complicated than the terrestrial planets. Nonetheless, enormous progress has been made over the last 25 years, thanks particularly to the *Galileo*, *Cassini* and *New Horizons* missions.

Many outstanding questions remain, however. A few specific ones that have been mentioned above are tabulated here:

| **Question** | **Section** |
|---|---|
| How thick is Europa's ice shell? | 1.2.2 |
| Does Europa really produce cryovolcanic plumes? | 2.1.5 |
| Why is Ganymede the only satellite with an internal dynamo? | 1.2.3 |
| Is Callisto really undifferentiated? | 1.2.3 |
| Why do the Galilean but not the Saturnian satellites show a regular density progression? | 3.2.1 |
| Are the Saturnian satellites young? | 3.2.3 |
| Why is Titan the only satellite with an extensive atmosphere? | 3.2.2 |
| How has Titan maintained a high orbital eccentricity? | 2.1.2 |
| What caused the activity on Miranda and Ariel? | 2.1.3 |
| Does Pluto have a subsurface ocean? | 1.2.7 |

:**Table 4**. Selected outstanding questions concerning icy satellite dynamics.

Planning for spacecraft missions to Europa and Ganymede by NASA and ESA, respectively, is quite well-advanced, so some of these questions should be definitively answered in the next decade or two. A future spacecraft mission to the Uranian satellites would vastly increase our knowledge of these enigmatic moons. And follow-up missions to both Titan and Enceladus are under active consideration.

As well as these specific questions, there are various areas of enquiry in which further study would be helpful. The dynamics of tidally-forced, ice-covered oceans (Section 2.1.2) is one such obvious topic, though what observations could be used to distinguish between different models is not clear. A closely-related topic - the rotational behaviour of bodies with subsurface oceans (Section 1.1.4) – is also ripe for more work and can potentially be tested using Earth-based radar (e.g. Margot et al. 2013). A broad – and difficult – topic is coupled thermal-orbital evolution (Section 3.1.2). The trick here is to integrate both geological and orbital observational constraints, and to try to develop a scenario which satisfies both. The main problem is the size of the parameter space (satellite $k_2/Q$, planetary $Q_p$, initial conditions . . .) which has to be explored. But only by considering both kinds of constraints together are answers likely to emerge. Lastly, it is likely that the next few years will herald the first "exo-moon" discovery, at which point all the expertise painstakingly developed in this solar system can be applied elsewhere.

References


Agnor, C.B. & Hamilton, D.P. (2006). Neptune's capture of its moon Triton in a binary-planet gravitational encounter, *Nature* 441, 192-194.

Anderson, J.D., Lau, E.L., Sjogren, W.L. et al. (1996). Gravitational constraints on the internal structure of Ganymede, *Nature* 384,541-543.

Anderson, J.D., Schubert, G., Jacobson, R.A. et al. (1998). Europa's differentiated internal structure: Inferences from four Galileo encounters, *Science* 285,2019-2022.

Anderson, J.D., Jacobson, R.A., McElrath, T.P. et al. (2001). Shape, mean radius, gravity field, and interior structure of Callisto, *Icarus* 153, 157-161.

Asphaug,. E., Reufer, A. (2013). Late origin of the Saturn system, *Icarus* 223, 544-565.

Baland, R.-M., Tobie, G., Lefevre, A. et al. (2014). Titan's internal structure inferred from its gravity field, shape, and rotation state. *Icarus* 237, 29-41.

Barr, A.C., Hammond, N.P. (2015). A common origin for ridge-and-trough terrain on icy satellites by sluggish lid convection, *Phys. Earth Planet. Inter.* 249, 18-27.

Barr, A.C., Citron, R.I., Canup, R.M. (2010). Origin of a partially differentiated Titan, *Icarus* 209,858-862.

Barr, A.C., Canup, R.M. (2010). Origin of the Ganymede-Callisto dichotomy by impacts during the late heavy bombardment, *Nature Geosci.* 3, 164-167.

Barr, A.C., Pappalardo, R.T., Zhong, S.J. (2004). Convective instability in ice I with non-Newtonian rheology: Application to the icy Galilean satellites, *J. Geophys. Res.* 109, E12008.

Behounkova, M., Tobie, G., Choblet, G., Cadek, O. (2012). Tidally-induced melting events as the origin of the south-pole activity on Enceladus. *Icarus* 219, 655-664.

Beuthe, M. (2013). Spatial patterns of tidal heating, *Icarus* 223, 308-329.

Beuthe, M., Rivoldini, A., Trinh, A. (2016). Enceladus's and Dione's floating ice shells supported by minimum stress isostasy, *Geophys. Res. Lett.* 43, 10088-10096.

Beuthe, M. (2016). Crustal control of dissipative ocean tides in Enceladus and other icy moons, *Icarus* 280, 278-299.

Billings, S.E., Kattenhorn, S.A. (2005). The great thickness debate: Ice shell thickness models for Europa and comparisons with estimates based on flexure at ridges, *Icarus* 177, 397-412.

Bills, B.G., Nimmo, F. (2011). Rotational dynamics and internal structure of Titan, *Icarus* 214, 351-355.

Bland, M.T., Singer, K.N., McKinnon, W.B. et al. (2017). Viscous relaxation of Ganymede's impact craters: Constraints on heat flux, *Icarus* 296, 275-288.

Bland, M.T., Singer, K.N., McKinnon, W.B. et al. (2012). Enceladus' extreme heat flux as revealed by its relaxed craters, *Geophys. Res. Lett.* 39,L17204.

Buie, M.W., Tholen, D.J., Grundy, W.M. (2012). The orbit of Charon is circular, *Astron. J.* 144, 15.

Canup, R.M. (2010). Origin of Saturn's rings and inner moons by mass removal from a lost Titan-sized satellite, *Nature* 468, 943-946.

Canup, R.M. (2005). A giant impact origin of Pluto-Charon, *Science* 307,546-550.

Canup, R.M., Ward, W.R. (2002). Formation of the Galilean satellites: Conditions of accretion, *Astron. J.* 124, 3404-3423.

Canup, R.M. & Ward, W.R. (2009). Origin of Europa and the Galilean satellites. In Pappalardo, R.T., McKinnon, W.B., Khurana, K. (eds.), *Europa*, pp.59-83, University of Arizona Press.

Canup, R.M., Ward, W.R. (2006). A common mass scaling for satellite systems of gaseous planets, *Nature* 441, 834-839.

Castillo-Rogez, J.C., Matson, D.L., Sotin, C. et al. (2007). Iapetus' geophysics: Rotation rate, shape, and equatorial ridge, *Icarus* 190,179-202.

Castillo-Rogez, J.C., Lunine, J.I. (2010). Evolution of Titan's rocky core constrained by Cassini observations. *Geophys. Res. Lett.* 37,L20205.

Castillo-Rogez, J.C., Hemingway, D., Tobie, G., McKinnon, W.B., & Schubert, G. (2018). Origin and evolution of Saturn's mid-sized moons, in Schenk, P.M., Clark, R.N., Howett, C.J.A., Verbiscer, A.J., Waite, J.H. *Enceladus and the icy moons of Saturn*. University of Arizona Press.

Charnoz, S., Morbidelli, A., Dones, L. et al. (2009). Did Saturn's rings form during the Late Heavy Bombardment? *Icarus* 199, 413-428.

Charnoz, S., Crida, A., Castillo-Rogez, J.C. et al. (2011). Accretion of Saturn's mid-sized moons during the viscous spreading of young massive rings: Solving the paradox of silicate-poor rings versus silicate-rich moons, *Icarus* 216, 535-550.

Chen, E.M.A., Nimmo, F., Glatzmaier, G.A. (2014). Tidal heating in icy satellite oceans, *Icarus* 229, 11-30.

Chen, E.M.A., Nimmo, F. (2008). Implications from Ithaca Chasma for the thermal and orbital history of Tethys, *Geophys. Res. Lett.* 35, L19203.

Choblet, G., Tobie, G., Sotin, C. et al. (2017). Powering prolonged hydrothermal activity inside Enceladus, *Nature Astron.* 1, 841-847.

Collins, G.C., McKinnon, W.B., Moore, J.M., Nimmo, F., Pappalardo, R.T., Prockter, L.M. & Schenk, P.M. (2010). Tectonics of the outer planet satellites. In T.R. Watters & R.A. Schultz (eds.), *Planetary Tectonics*, pp. 233-263, Cambridge University Press.

Crawford, G.D., Stevenson, D.J. (1988). Gas-driven water volcanism and the resurfacing of Europa, *Icarus* 73, 66-79.

Croft, S.K., Kargel, J.S., Kirk, R.L. et al. (1995). The geology of Triton. In D.P. Cruikshank (ed.), *Neptune and Triton*, pp.879-947, Univ. Arizona Press.

Cuk, M., Dones, L., Nesvorny, D. (2016). Dynamical evidence for a late formation of Saturn's moons, *Astrophys. J.* 820, 97.

Davies, M.E., Colvin, T.R., Oberts, J. et al. (1998). The control networks of the Galilean satellites and implications for global shape, *Icarus* 135, 372-376.

Dermott, S.F., Malhotra, R., Murray, C.D. (1988). Dynamics of the Uranian and Saturnian satellite systems – a chaotic route to melting Miranda. *Icarus* 76, 295-334.

Dombard, A.J., Patterson, G.W., Lederer, A.P. et al. (2013). Flanking fractures and the formation of double ridges on Europa, *Icarus* 223, 74-81.

Dones, L., Chapman, C.R., McKinnon, W.B., Melosh, H.J., Kirchoff, M.R., Neukum, G. & Zahnle, K.J. (2009). Icy satellites of Saturn: Impact cratering and age determination. In M.K. Dougherty, L.W. Esposito & S. M. Krimigis (eds.), *Saturn from Cassini-Huygens*, pp. 613-636, Springer

Dwyer, C.A., Nimmo, F., Ogihara, M. et al. (2013). The influence of imperfect accretion and radial mixing on ice: rock ratios in the Galilean satellites, *Icarus* 225, 390-402.

Fagents, S.A. (2003). Considerations for effusive cryovolcanism on Europa: The post-Galileo perspective, *J. Geophys. Res.* 108, 5139.

Fuller, J., Luan, J., Quataert, E. (2016). Resonance locking as the source of rapid tidal migration in the Jupiter and Saturn moon systems, *Mon. Not. R. Astron. Soc.* 458, 3867-3879.

Giese, B., Wagner, R., Neukum, G. et al. (2007). Tethys: Lithospheric thickness and heat flux from flexurally supported topography at Ithaca Chasma, *Geophys. Res. Lett.* 34, L21203.

Giese, B., Wagner, R., Hussmann, H. et al. (2008). Enceladus: An estimate of heat flux and lithospheric thickness from flexurally supported topography, *Geophys. Res. Lett.* 35, L24204.

Giese, B., Denk, T., Neukum, G. et al. (2008). The topography of Iapetus' leading side, *Icarus* 193, 359-371.

Goldsby, D.L., Kohlstedt, D.L. (2001). Superplastic deformation of ice: Experimental observations, *J. Geophys. Res.* 106, 11017-11030.

Goldreich, P., Murray, N., Longaretti, P.Y. et al. (1989). Neptune's story. *Science* 245, 500-504.

Goldreich, P., Mitchell, J.L. (2010). Elastic ice shells of synchronous moons: Implications for cracks on Europa and non-synchronous rotation of Titan. *Icarus* 209, 631-638.

Greenberg, R., Geissler, P., Hoppa, G. et al. (2002). Tidal-tectonic processes and their implications for the character of Europa's icy crust, *Rev. Geophys.* 40, 1004.

Greenberg, R., Weidenschilling, S.J. (1984). How fast do Galilean satellites spin? *Icarus* 58, 186-196.

Griffith, C.A., Zahnle, K. (1995). Influx of cometary volatiles to planetary moons – the atmospheres of 1000 possible Titans, *J. Geophys. Res.* 100, 16907-16922.

Hammond, N. P., Phillips, C. B., Nimmo, F., et al. (2013). Flexure on Dione: Investigating subsurface structure and thermal history, *Icarus* 223,418-422.

Hauck, S.A., Aurnou, J.M., Dombard, A.J. (2006). Sulfur's impact on core evolution and magnetic field generation on Ganymede, *J. Geophys. Res.* 111, E09008.

Hedman, M. M., Gosmeyer, C. M., Nicholson, P. D., et al. (2013). An observed correlation between plume activity and tidal stresses on Enceladus, *Nature* 500, 182-184.

Hemingway, D.J., Zannoni, M., Tortora, P. et al. (2016). Dione's Internal Structure Inferred from Cassini Gravity and Topography, *47th Lunar and Planetary Science Conference*, Abstract #1314.

Hemingway, D., Nimmo, F., Zebker, H., et al. (2013). A rigid and weathered ice shell on Titan, *Nature* 500, 550-552.

Hemingway, D., Iess, L., Tajeddine, R., Tobie, G. (2018). The interior of Enceladus, in Schenk, P.M., Clark, R.N., Howett, C.J.A., Verbiscer, A.J., Waite, J.H. *Enceladus and the icy moons of Saturn*. University of Arizona Press.

Hirata, N. (2016). Differential impact cratering of Saturn's satellites by heliocentric impactors, *J. Geophys. Res.* 121, 111-117.

Hoppa, GV, Tufts, BR, Greenberg, R, et al. (1999b). Formation of cycloidal features on Europa, *Science* 285, 1899-1902.

Hoppa, G, Greenberg, R, Geissler, P, et al. (1999a) Rotation of Europa: Constraints from terminator and limb positions, *Icarus* 137, 341-347.

Hsu, H.-W., Postberg, F., Sekine, Y. et al. (2015). Ongoing hydrothermal activities within Enceladus, *Nature* 519, 207-210.

Hurford, T. A., Helfenstein, P., Hoppa, G. V., et al. (2007). Eruptions arising from tidally controlled periodic openings of rifts on Enceladus, *Nature* 447, 292-294.

Hussmann, H, Spohn, T, Wieczerkowski, K. (2002). Thermal equilibrium states of Europa's ice shell: Implications for internal ocean thickness and surface heat flow, *Icarus* 156, 143-151.

Hussmann, H., Sohl, F., Spohn, T. (2006). Subsurface oceans and deep interiors of medium-sized outer planet satellites and large trans-neptunian objects, *Icarus* 185, 258-273.

Hussmann, H, Spohn, T. (2004). Thermal-orbital evolution of Io and Europa, *Icarus* 171, 391-410.

Iess, L., Stevenson, D. J., Parisi, M., et al. (2014). The Gravity Field and Interior Structure of Enceladus , *Science* 344, 78-80.

Iess, L., Jacobson, R.A., Ducci, M. et al. (2012). The Tides of Titan, *Science* 337, 457-459.

Iess, L., Rappaport, N.J., Jacobson, R.A. et al. (2010). Gravity Field, Shape, and Moment of Inertia of Titan, *Science* 327, 1367-1369.

Ingersoll, A.P., Ewald, S.P. (2017). Decadal timescale variability of the Enceladus plumes inferred from Cassini images, *Icarus* 282, 260-275.

Kargel, J.S. (1998). Physical chemistry of ices in the outer solar system. In B. Schmitt, C. De Bergh & M. Festou (eds.), *Solar System Ices*, pp.3-32, Kluwer.

Keane, J.T., Matsuyama, I., Kamata, S. et al. (2016). Reorientation and faulting of Pluto due to volatile loading within Sputnik Planitia, *Nature* 540, 90-93.

Khurana, KK, Kivelson, MG, Russell, CT. (2002). Searching for liquid water in Europa by using surface observatories, *Astrobiology* 2, 93-103.

Kirk, R.L., Soderblom, L.A., Brown, R.H., Kieffer, S.W., Kargel, J.S. (1995), Triton’s plumes: discovery, characteristics, and models, in D.P. Cruikshank (ed.), *Neptune and Triton*, pp. 949-990, Univ. Arizona Press.

Kivelson, MG, Khurana, KK, Volwerk, M (2002). The permanent and inductive magnetic moments of Ganymede, *Icarus* 157, 507-522.

Lainey, V., Jacobson, R.A., Tajeddine, R. et al. (2017). New constraints on Saturn’s interior from Cassini astrometric data. *Icarus* 281, 286-296.

Lainey V., Arlot, J.E., Karatekin, O. et al. (2009). Strong tidal dissipation in Io and Jupiter from astrometric observations, *Nature* 459, 957-959.

Leliwa-Kopystynski, J., Maruyama, M., Nakajima, T. (2002). The water-ammonia phase diagram up to 300 MPa: Application to icy satellites, *Icarus* 159, 518-528.

Lopes, R. M. C., Kirk, R. L., Mitchell, K. L., et al. (2013). Cryovolcanism on Titan: New results from Cassini RADAR and VIMS, *J. Geopys. Res.* 118, 416-435.

Lorenz, R.D., Stiles, B.W., Kirk, R.L. et al. (2008). Titan's rotation reveals an internal ocean and changing zonal winds, *Science* 319, 1649-1651.

McKinnon, WB (1997). Mystery of Callisto: Is it undifferentiated? *Icarus* 130, 540-543.

McKinnon, W.B., Stern, S.A., Weaver, H.A. et al. (2017). Origin of the Pluto-Charon system: Constraints from the New Horizons flyby, *Icarus* 287, 2-11.

McKinnon, W.B., Nimmo, F., Wong, T. et al. (2016). Convection in a volatile nitrogen-ice-rich layer drives Pluto's geological vigour, *Nature* 534, 82-84.

McKinnon, W.B. (1998). Geodynamics of icy satellites. In B. Schmitt, C. De Bergh & M. Festou (eds.), *Solar System Ices*, pp.525-550, Kluwer.

Manga, M., Wang, C.-Y. (2007). Pressurized oceans and the eruption of liquid water on Europa and Enceladus, *Geophys. Res. Lett.* 34, L07202.

Manga, M., Michaut, C. (2017). Formation of lenticulae on Europa by saucer-shaped sills, *Icarus* 286, 261-269.

Margot, J.L., Padovan, S., Campbell, D., Peale, S. & Ghigo, F. (2013). Measurements of the spin states of Europa and Ganymede, *Division Planet. Sci. Mtg. Abs.* 45, 50402.

Marzari, F, Dotto, E, Davis, DR, et al. (1998). Modelling the disruption and reaccumulation of Miranda, *Astron. Astrophys.* 333, 1082-1091.

Matson, D.L., Castillo-Rogez, J.C., Schubert, G., Sotin, C. & McKinnon, W.B. (2009). The thermal evolution and internal structure of Saturn's mid-sized icy satellites. In M.K. Dougherty, L.W. Esposito & S. M. Krimigis (eds.), *Saturn from Cassini-Huygens*, pp. 613-636, Springer.

Matsuyama, I., Nimmo, F. (2008). Tectonic patterns on reoriented and despun planetary bodies, *Icarus* 195, 459-473.

Melosh, H.J. (1989). *Impact cratering: a geologic process*. Oxford University Press.

Meyer, J., Wisdom, J. (2008). Tidal evolution of Mimas, Enceladus, and Dione, *Icarus* 193, 213-223.

Meyer, J., Wisdom, J. (2007). Tidal heating in Enceladus, *Icarus* 188, 535-539.

Moore, WB, Schubert, G (2000).The tidal response of Europa, *Icarus* 147, 317-319.

Moore, J.M., McKinnon, W.B., Spencer, J.R. et al. (2016). The geology of Pluto and Charon through the eyes of New Horizons, *Science* 351, 1284-1293.

Moore, J.M., Pappalardo, R.T. (2011). Titan: An exogenic world? *Icarus* 212, 790-806.

Morbidelli, A., Marchi, S., Bottke, W. F., et al. (2012). A sawtooth-like timeline for the first billion years of lunar bombardment, *Earth Planet. Sci. Lett.* 355, 144-151.

Mosqueira, I, Estrada, PR (2003). Formation of the regular satellites of giant planets in an extended gaseous nebula I: subnebula model and accretion of satellites, *Icarus* 163, 198-231.

Movshovitz, N., Nimmo, F., Korycansky, D. G., et al. (2015). Disruption and reaccretion of midsized moons during an outer solar system Late Heavy Bombardment, *Geophys. Res. Lett.* 42, 256-263.

Murray, C.D., Dermott, S.F. (1999). *Solar system dynamics*. Cambridge University Press.

Muller-Wodarg, I., Griffith, C.A., Lellouch, E. & Cravens, T.E. (2014). *Titan*. Cambridge University Press.

Nagel, K, Breuer, D, Spohn, T (2004). A model for the interior structure, evolution, and differentiation of Callisto, *Icarus* 169, 402-412.

Nesvorny, D., Youdin, A.N., Richardson, D.C. (2010). Formation of Kuiper Belt binaries by gravitational collapse, *Astron. J.* 140, 785-793.

Nimmo, F, Pappalardo, RT, Giese, B (2002). Effective elastic thickness and heat flux estimates on Ganymede, *Geophys. Res. Lett.* 29, 1158.

Nimmo, F. (2004). Stresses generated in cooling viscoelastic ice shells: Application to Europa, *J. Geophys. Res.* 109, E12001.

Nimmo, F., Pappalardo, R.T. (2006). Diapir-induced reorientation of Saturn's moon Enceladus, *Nature* 441, 614-616.

Nimmo, F., Matsuyama, I. (2007). Reorientation of icy satellites by impact basins, *Geophys. Res. Lett.* 34, L19203.

Nimmo, F., Thomas, P. C., Pappalardo, R. T., et al. (2007). The global shape of Europa: Constraints on lateral shell thickness variations, *Icarus* 191, 183-192.

Nimmo, F., Bills, B. G. (2010). Shell thickness variations and the long-wavelength topography of Titan, *Icarus* 208, 896-904.

Nimmo, F., Bills, B. G., Thomas, P. C. (2011). Geophysical implications of the long-wavelength topography of the Saturnian satellites, *J. Geophys. Res.* 116, E11001.

Nimmo, F., Porco, C., Mitchell, C. (2014). Tidally-modulated eruptions on Enceladus: Cassini ISS observations and models, *Astron. J.* 148, 46.

Nimmo, F. & Pappalardo, R.T. (2016). Ocean worlds in the outer solar system, *J. Geophys. Res.* 121, 1378-1399.

Nimmo, F., Hamilton, D. P., McKinnon, W. B., et al. (2016). Reorientation of Sputnik Planitia implies a subsurface ocean on Pluto, *Nature* 540, 94-96.

Nimmo, F., Umurhan, O., Lisse, C.M. et al. (2017). Mean radius and shape of Pluto and Charon from New Horizons images, *Icarus* 287, 12-29.

Nimmo, F., Barr, A.C., Behounkova, M., McKinnon, W.B. (2018). The thermal and orbital evolution of Enceladus: observational constraints and models, in Schenk, P.M., Clark, R.N., Howett, C.J.A., Verbiscer, A.J., Waite, J.H. *Enceladus and the icy moons of Saturn*. University of Arizona Press.

Ogihara, M., Ida, S. (2012). N-body simulations of satellite formation around giant planets: origin of orbital configuration of the Galilean moons, *Astrophys. J.* 753, 60.

Ojakangas, G.W., Stevenson, D.J. (1989). Thermal state of an ice shell on Europa, *Icarus* 81, 220-241.

Ojakangas, G.W., Stevenson, D.J. (1986). Episodic volcanism of tidally heated satellites with application to Io, *Icarus* 66, 341-358.

Palguta, J, Anderson, JD, Schubert, G, et al. (2006). Mass anomalies on Ganymede, *Icarus* 180, 428-441.

Pappalardo, RT, Reynolds, SJ, Greeley, R (1997). Extensional tilt blocks on Miranda: Evidence for an upwelling origin of Arden Corona, *J. Geophys. Res.* 102, 13369-13379.

Pappalardo, R.T., McKinnon, W.B., Khurana, K. (2009). *Europa*. University of Arizona Press.

Peale, S.J. (1999). Origin and evolution of the natural satellites, *Ann. Rev. Astron. Astrophys.* 37, 533-602.

Peterson, G., Nimmo, F., Schenk, P. (2015). Elastic thickness and heat flux estimates for the uranian satellite Ariel, *Icarus* 250, 116-122.

Porco, CC, Helfenstein, P, Thomas, PC, et al. (2006). Cassini observes the active South Pole of Enceladus, *Science* 311, 1393-1401.

Postberg, F., Schmidt, J., Hillier, J., et al. (2011). A salt-water reservoir as the source of a compositionally stratified plume on Enceladus, *Nature* 474, 620-622.

Rhoden, A.R., Hurford, T.A. (2013). Lineament azimuths on Europa: Implications for obliquity and non-synchronous rotation, *Icarus* 226, 841-859.

Rhoden, A.R., Henning, W., Hurford, T.A. (2015). The interior and orbital evolution of Charon as preserved in its geologic record, *Icarus* 246, 11-20.

Roberts, J.H. (2015). The fluffy core of Enceladus, *Icarus* 258, 54-66.

Robuchon, G., Nimmo, F. (2011). Thermal evolution of Pluto and implications for surface tectonics and a subsurface ocean, *Icarus* 216, 426-439.

Ronnet, T., Mousis, O., Vernazza, P. (2017). Pebble Accretion at the Origin of Water in Europa, *Astrophys. J.* 892, 92.

Ross, R.G. & Kargel, J.S. (1998). Thermal conductivity of solar system ices, with special reference to Martian polar caps. In B. Schmitt, C. De Bergh & M. Festou (eds.), *Solar System Ices*, pp.33-62, Kluwer.

Roth, L., Saur, J., Retherford, K.D. et al. (2014). Transient Water Vapor at Europa's South Pole *Science* 343, 171-174.

Schenk, P.M. (1991). Fluid volcanism on Miranda and Ariel – flow morphology and composition, *J. Geophys. Res.* 96, 1887-1906.

Schenk, P., Jackson, M.P.A. (1993). Diapirism on Triton – a record of crustal layering and instability, *Geology* 21, 299-302.

Schenk, P.M., McKinnon, W.B., Gwynn, D. et al. (2001). Flooding of Ganymede's bright terrains by low-viscosity water-ice lavas, *Nature* 410, 57-60.

Schenk, P.M. (2002). Thickness constraints on the icy shells of the galilean satellites from a comparison of crater shapes, *Nature* 417, 419-421.

Schenk, P.M., Matsuyama, I., Nimmo, F. (2008). True polar wander on Europa from global-scale small-circle depressions, *Nature* 453, 368-371.

Schenk, P.M., Clark, R.N., Howett, C.J.A., Verbiscer, A.J., Waite, J.H. (2018). *Enceladus and the icy moons of Saturn*. University of Arizona Press.

Schubert, G., Anderson, J.D., Spohn, T. & McKinnon, W.B. (2004). Interior composition, structure and dynamics of the Galilean satellites. In F. Bagenal, T. Dowling & W. McKinnon (eds.), *Jupiter*, pp. 281-306, Cambridge University Press.

Sekine, Y., Genda, H. (2012). Giant impacts in the Saturnian system: A possible origin of diversity in the inner mid-sized satellites, *Planetary Space Sci.* 63-64, 133-138.

Shoji, D., Hussmann, H., Sohl, F., Kurita, K. (2014). Non-steady state tidal heating of Enceladus, *Icarus* 235, 75-85.

Showman, AP, Malhotra, R. (1997). Tidal evolution into the Laplace resonance and the resurfacing of Ganymede, *Icarus* 127, 93-111.

Showman, AP, Mosqueira, I, Head, JW, (2004). On the resurfacing of Ganymede by liquid-water volcanism, *Icarus* 172, 625-640.

Showman, A.P., Han, L.J. (2005). Effects of plasticity on convection in an ice shell: Implications for Europa. *Icarus* 177, 425-437.

Sohl, F, Hussmann, H, Schwentker, B, et al. (2003). Interior structure models and tidal Love numbers of Titan, *J. Geophys. Res.* 108, 5130.

Solomatov, V.S. (1995). Scaling of temperature-dependent and stress-dependent viscosity convection, *Phys. Fluids* 7, 266-274.

Sotin, C, Head, JW, Tobie, G. (2002). Europa: Tidal heating of upwelling thermal plumes and the origin of lenticulae and chaos melting, *Geophys. Res. Lett.* 29, 1233.

Sotin, C., Grasset, O. & Beauchesne, S. (1998). Thermodynamical properties of high pressure ices. Implications for the dynamics and internal structure of large icy satellites. In B. Schmitt, C. De Bergh & M. Festou (eds.), *Solar System Ices*, pp.79-96, Kluwer.

Sparks, W. B., Schmidt, B. E., McGrath, M. A., et al. (2017). Active Cryovolcanism on Europa? *Astrophys. J.* 839, L18.

Spencer, JR, Pearl, JC, Segura, M, et al. (2006). Cassini encounters Enceladus: Background and the discovery of a south polar hot spot, *Science* 311, 1401-1405.

Spencer, J.R., Nimmo, F., Ingersoll, A.P., Hurford, T.A., Kite, E.S., Rhoden, A.R., Schmidt, J., Howett, C.J.A. (2018). Plume origins and plumbing (ocean to surface), in Schenk, P.M., Clark, R.N., Howett, C.J.A., Verbiscer, A.J., Waite, J.H. *Enceladus and the icy moons of Saturn*. University of Arizona Press.

Stacey, F.D. (1969). *Physics of the Earth*. John Wiley & Sons, New York.

Stiles, B.W., Kirk, R.L., Lorenz, R.D. et al. (2008). Determining Titan's spin state from Cassini RADAR images, *Astron. J.* 135, 1669-1680.

Sqyures, S.W., Reynolds, R.T., Summers, A.L. et al. (1988). Accretional heating of the satellites of Saturn and Uranus, *J. Geophys. Res.* 93, 8779-8794.

Tackley, P.J. (2000). Mantle convection and plate tectonics: Toward an integrated physical and chemical theory. *Science* 288, 2002-2007.

Tajeddine, R., Rambaux, N., Lainey, V., et al. (2014). Constraints on Mimas' interior from Cassini ISS libration measurements, *Science* 346, 322-324.

Thomas, P.C. (1988). Radii, shapes and topography of the satellites of Uranus from limb coordinates, *Icarus* 73, 427-441.

Thomas, P.C. (2000). The shape of Triton from limb profiles, *Icarus* 148, 587-588.

Thomas, P. C. (2010). Sizes, shapes, and derived properties of the saturnian satellites after the Cassini nominal mission, *Icarus* 208, 395-401.

Thomas, P. C., Tajeddine, R., Tiscareno, M. S., et al. (2016). Enceladus's measured physical libration requires a global subsurface ocean, *Icarus* 264, 37-47.

Tiscareno, M.S., Thomas, P.C., Burns, J.A. (2009). The rotation of Janus and Epimetheus, *Icarus* 204, 254-261.

Tobie, G, Mocquet, A, Sotin, C (2005). Tidal dissipation within large icy satellites: Applications to Europa and Titan, *Icarus* 177, 534-549.

Tobie, G., Lunine, J.I., Monteux, J., Mousis, O. & Nimmo, F. (2014). The origin and evolution of Titan. In I. Muller-Wodarg, C.A. Griffith, E. Lellouch & T.E. Cravens (eds.), *Titan*, pp. 29-62, Cambridge University Press, New York, USA.

Tortora, P., Zannoni, M., Hemingway, D. et al. (2016). Rhea gravity field and interior modeling from Cassini data analysis, *Icarus* 264, 264-273.

Tricarico, P. (2014). Multilayer hydrostatic equilibrium of planets and synchronous moons: Theory and application to Ceres and to solar system moons. *Astrophys. J.* 782, 99.

Turcotte, D.L., Schubert, G. (2002). *Geodynamics* (2nd ed.). Cambridge University Press.

Turtle, EP, Pierazzo, E (2001). Thickness of a European ice shell from impact crater simulations, *Science* 294, 1326-1328.

Tyler, R.H. (2008). Strong ocean tidal flow and heating on moons of the outer planets, *Nature* 456, 770-772.

Van Hoolst, T., Baland, R.-M., Trinh, A. (2013). On the librations and tides of large icy satellites, *Icarus* 226, 299-315.

Wahr, J. M., Zuber, M. T., Smith, D. E., et al. (2006). Tides on Europa, and the thickness of Europa's icy shell, *J. Geophys. Res.* 111, E12005.

Waite, J.H., Glein, C.R., Perryman, R.S. et al. (2017). Cassini finds molecular hydrogen in the Enceladus plume: Evidence for hydrothermal processes. *Science* 356, 155-159.

Ward, W.R., Canup, R.M. (2010). Circumplanetary disk formation. *Astron. J.* 140, 1168-1193.

White, O.L., Schenk, P.M., Dombard, A.J. (2013). Impact basin relaxation on Rhea and Iapetus and relation to past heat flow, *Icarus* 223, 699-709.

White, O.L., Schenk, P.M., Bellagamba, A.W. et al. (2017). Impact crater relaxation on Dione and Tethys and relation to past heat flow, *Icarus* 288, 37-52.

Wisdom, J. (2008). Tidal dissipation at arbitrary eccentricity and obliquity, *Icarus* 193, 637-640.

Zahnle, K, Schenk, P, Sobieszczyk, S, et al. (2001). Differential cratering of synchronously rotating satellites by ecliptic comets, *Icarus* 153, 111-129.

Zahnle, K, Schenk, P, Levison, H, et al. (2003). Cratering rates in the outer Solar System, *Icarus* 163, 263-289.

Zebker, H.A., Stiles, B., Hensley, S. et al. (2009). Size and Shape of Saturn's Moon Titan, *Science* 324, 921-923.

Zhang, K., Nimmo, F. (2012). Late-stage impacts and the orbital and thermal evolution of Tethys, *Icarus* 218, 348-355.

Zimmer, C, Khurana, KK, Kivelson, MG (2000). Subsurface oceans on Europa and Callisto: Constraints from Galileo magnetometer observations, *Icarus* 147, 329-347.

Further Reading

Bagenal, F., Dowling, T. & McKinnon, W. (eds.) (2007), *Jupiter*, Cambridge University Press.

Cruikshank, D.P., (ed.) (1995), *Neptune and Triton*, Univ. Arizona Press.

Dougherty, M.K., Esposito, L.W., & Krimigis, S.M. (eds.) (2009), *Saturn from Cassini-Huygens*, Springer

Melosh, H.J. (1989). *Impact cratering: a geologic process*. Oxford University Press.

Muller-Wodarg, I., Griffith, C.A., Lellouch, E. & Cravens, T.E. (2014). *Titan*. Cambridge University Press.

Murray, C.D., Dermott, S.F. (1999). *Solar system dynamics*. Cambridge University Press.

Nimmo, F. & Pappalardo, R.T. (2016). Ocean worlds in the outer solar system, *J. Geophys. Res.* 121, 1378-1399.

Pappalardo, R.T., McKinnon, W.B., Khurana, K. (eds.) (2009), *Europa*, University of Arizona Press.

Peale, S.J. (1999). Origin and evolution of the natural satellites, *Ann. Rev. Astron. Astrophys.* 37, 533-602.

Schenk, P.M., Clark, R.N., Howett, C.J.A., Verbiscer, A.J., Waite, J.H. (eds.) (2018) *Enceladus and the icy moons of Saturn*. University of Arizona Press.

Schmitt, B., De Bergh, C. & Festou, M. (eds.) (1998), *Solar System Ices*, Kluwer.

Turcotte, D.L., Schubert, G. (2002). *Geodynamics* (2nd ed.). Cambridge University Press.

Watters, T.R. & Schultz, R.A. (eds.) (2010), *Planetary Tectonics*, Cambridge University Press.